

Report on metal content mobilisation with nanoparticles

CHPM2030 Deliverable D2.3

Version: June 2018



Author contact

Steven Mullens

VITO

Boeretang 200

2400 MOL

Belgium

Email: steven.mullens@vito.be

Published by the CHPM2030 project, 2018

University of Miskolc

H-3515 Miskolc-Egyetemváros

Hungary

Email: foldshe@uni-miskolc.hu



CHPM2030 DELIVERABLE D2.3

REPORT ON METAL CONTENT MOBILISATION WITH NANOPARTICLES

Summary:

The surface of activated carbon particles has been modified in order to increase their sorption performance for a variety of valuable metal ions. Different strategies for the surface modification allow a variety of metal to be sorbed, both in acid and alkaline pH regions.

The permeability of the carbon particles in a porous structure has been investigated as function of the pore size distribution.

Authors:

S. Mullens, VITO, researcher
E. Moens, VITO, lab technician
R. Kemps, VITO, SEM analysis
A. de Wilde, VITO, Analytical lab
W. Brusten, VITO, Analytical lab
W. Bouwen, VITO, technician
A. Claes, VITO, lab technician

This project has received funding from the European Union's Horizon 2020 research and innovation programme under grant agreement n° 654100.



TABLE OF CONTENTS

Contents

1	Executive summary	8
2	Introduction	9
	Objectives	9
	Research strategy	9
3	Surface modification	13
	Objectives	13
	Screening and selection of activated carbon powders	13
3.1	Literature overview	13
3.2	Screening and selection of activated carbon powders	17
3.3	Characterisation of activated carbon powders	19
	Surface modification of activated carbon powders	26
3.4	Selection of surface modification technologies	26
3.5	Acidic treatment	28
3.6	Surface modification by atmospheric plasma treatment	34
4	Sorption performance	38
	Objectives	38
	Research approach	38
	Model sorption performance	39
4.1	Experimental set-up	39
4.2	Sorption kinetics	40
4.3	Solid-to-liquid ratio	42
4.4	pH range	44
4.5	Influence of the Nd starting concentration	46
	Competitive sorption performance	48
4.6	Competitive sorption with other rare earth elements	48
4.7	Competitive sorption with common metal ions	49
	Sorption performance under more extreme conditions	52
4.8	Influence of temperature, salinity and competitive common metal ion	52
5	Permeability	55
	Objectives	55
	Research approach	55
5.1	Experimental set-up	55
5.2	Screening and selection of simulated rock samples	57
5.3	Permeability experiments	62
6	References	67
7	Conclusions	69

LIST OF FIGURES

Figure 1: Research strategy.....	12
Figure 2 : Schematic representation of the structure of activated carbon, showing different oxygen surface groups.....	13
Figure 3 : Schematic view of some acidic (red) and alkaline (blue) surface groups with different heteroatoms bonded to aromatic rings on activated carbon.	14
Figure 4 : Classification of the approaches for surface modification of activated carbons.	15
Figure 5 : Cation exchange mechanism with carbon surface carboxylic group.	16
Figure 6 : TGA-MS equipment, with MS (left) and TGA coupled to a gas panel.....	21
Figure 7 : TGA-MS analysis of 2 activated carbons before surface modification : Norit CA-1 (left) and Kuraray YP-50F (right).	22
Figure 8 : IR-ATR equipment	23
Figure 9 : IR-ATR spectra of activated carbons before surface modification.	23
Figure 10 : Equipment used for measurement of the zeta potential.	24
Figure 11 : Principle of the element analyser and equipment.	25
Figure 12 : Overview of materials and surface modification approaches.	27
Figure 13 : Experimental set-up for the acidic treatment of activated carbon.....	28
Figure 14 : Flow chart for the acidic treatment of activated carbon.....	29
Figure 15 : TGA-MS of Norit CA1 before (black, dotted lines m/z) and after (red, full line m/z) acidic surface modification.	31
Figure 16 : TGA-MS of Kuraray YP50F before (black, dotted lines m/z) and after (red, full line m/z) acidic surface modification.	32
Figure 17 : IR-ATR spectra of Norit activated carbons before and after acidic surface modification.	33
Figure 18 : Plasmazone reactor.....	34
Figure 19 : Schematic representation of the AP reactor (Plazooka) used for powder functionalisation.	35
Figure 20 : TGA-MS analysis of activated carbon powders before and after AP-functionalisation (i) Norit and (ii) Kuraray.....	36
Figure 21 : Mass spectrum of allyl amine (electron ionisation, NIST webbook)	37
Figure 22 : Example of an elemental composition of leachate using acetic acid	38
Figure 23 : Experimental set-up for measuring the sorption performance.	39
Figure 24 : Speciation diagrams for neodymium as function of the pH.	40
Figure 25 : Nd adsorption as function of time for activated carbon Norit before and after acidic functionalisation.	42
Figure 26 : Nd sorption as function of the solid-to-liquid ratio for activated carbons after acidic functionalisation.	44
Figure 27 : Nd sorption as function of pH for activated carbon Norit before and after acidic functionalisation.	45
Figure 28 : Nd sorption as function of the origin Nd concentration for activated carbons after acidic functionalisation.	47
Figure 29 : Nd, Ce and La sorption as function of pH for (i) activated carbon Norit before and (ii) after acidic functionalisation.	49
Figure 30 : Speciation diagram for Pb.....	49
Figure 31 : Experimental set-up for measuring the sorption performance at higher temperatures.	52
Figure 32 : Experimental set-up for measuring the permeability	56

Figure 33 : Typical sample holder for measuring permeability of thin sheet membranes.	57
Figure 34 : Hg porosimetry analysis of sample 1.	58
Figure 35 : SEM analysis of sample 1: surface (top left) and fracture surface (top right, bottom)...	59
Figure 36 : Hg porosimetry analysis of sample 2.	60
Figure 37 : SEM analysis of sample 2: surface (top left) and fracture surface (top right, bottom)...	60
Figure 38 : Hg porosimetry analysis of sample 3.	61
Figure 39 : SEM analysis of sample 3: surface (top left) and fracture surface (top right, bottom)...	62
Figure 40 : Permeability set-up and mounting a porous sample in the holder.....	62
Figure 41 : Outcome of a typical permeability experiment of a porous ceramic.....	63
Figure 42 : Evolution of weight of the permeate and calculated flux over time for sample 3 (carbon suspension, 2 bar)	64
Figure 43 : The flow of the permeate for sample 3 (sample thickness 2.5 cm (left) and 0.4 cm (right)).	65
Figure 44 : Top view on sample 3 after permeability experiment.	65

LIST OF TABLES

Table 1 : Overview of the analytical tools used for the characterisation of the activated carbon powders.....	17
Table 2 : Overview of material properties of the activated carbon powders.	18
Table 3 : Thermal stability of functional groups on activated carbon and products formed during decomposition.	20
Table 4 : Interpretation and attribution of absorbance peaks in the IR-ATR spectra of activated carbons.....	24
Table 5 : Elemental composition of the Norit activated carbon powder.	25
Table 6 : Overview of the structural parameters of the 2 activated carbons before and after acidic treatment, as measured by N ₂ -sorption.	30
Table 7 : Elemental composition and contact pH of Norit activated carbon before and after acidic treatment.	33
Table 8 : Experimental conditions for AP-functionalisation of activated carbon powders.....	35
Table 9 : Contact pH values for activated carbons before and after AP-functionalisation.....	37
Table 10 : Evolution of pH as function of adsorption time for Norit activated carbon before and after modification.	41
Table 11 : Evolution of pH as function of the solid-to-liquid ratio for the activated carbons after acidic treatment.....	43
Table 12 : Concentration of metals in filtrate and adsorption percentage of Nd, Ce, La and Pb for Norit activated carbon and the activated carbons after acidic treatment.....	50
Table 13 : Concentration of metals in filtrate and adsorption percentage of Nd, Ce, La and Pb for Norit activated carbon and the activated carbons after acidic treatment.(sorption conditions: 80°C, 0.5M NaCl).	53
Table 14 : Overview of materials used for permeability tests.....	57
Table 15 : Water flux for the 3 samples.....	64

1 Executive summary

The CHPM2030 project aims to develop a novel technological solution of Combined Heat, Power and Metal (CHPM) extraction from ultra-deep ore bodies, that will pave the way for pilot-scale systems to be operational by 2030. This technology will help increase the attractiveness of renewable geothermal energy and also reduce Europe's dependency on the import of metals and fossil fuels. In the envisioned technology, an engineered geothermal system (EGS) is established within a metal-bearing geological formation at depths of 4 km or more, which will be manipulated in such a way that the co-production of energy and metals will be possible.

Here we report research focussed on the separation and recovery of specific metals which are present in the EGS fluids. The aim of this study was to demonstrate the feasibility of using carbon particles as sorbent materials for these metals. Furthermore, by tuning the surface chemistry of these carbon particles we aim to target specific metal ions released by in situ leaching. Two approaches for tuning the surface chemistry were explored, enabling the functionalisation of the carbon surface with acidic or alkaline groups. As such a wide variety of metals, or experimental conditions with regard to pH could be targeted.

The selection of rare earth elements as the main class of targeted metals was supported by their top ranking on the list of critical raw materials, as published by the European Commission in 2017. Due to the chemical nature of the rare earth elements, the sorbents with acidic functionalisation were selected for a full material characterisation and to demonstrate their sorption performance.

We demonstrate the importance of the carbon characteristics for the functionalisation and the nature of acidic groups formed. Although a fully quantitative analysis of the surface chemistry proved difficult, differences in sorption performance between different carbon particles for neodymium (Nd) as a model rare earth element were clearly identified. The best performing powder had adsorption percentages above 90 %. It was demonstrated that the trends observed for Nd were also valid for other rare earth elements.

We also found that the surface functionalisation changed the nature of the sorption performance. In some cases this resulted in a broader pH range over which metal sorption occurred, which might facilitate metal capture over a wider range of natural environments. However, in some cases this also resulted in a decrease in overall sorption capacity.

The competition in sorption with other metal ions which are present in higher concentration (Pb) was investigated as well. As the concentration of these metal ions increased, the sorption capacity for rare earth elements decreased, although not to the same extent for all powders. Functionalised powder had still a significant sorption capacity (~40 %) at relevant Pb concentrations (1000 ppm).

More negative impact on the sorption behaviour was observed when performing the experiments at a combination of high temperature (80°C), high salinity (0.5 M) and high competition with other metals (Pb), with sorption percentages in the range of 20 – 30 %.

Envisioning the CHPM2030 concept in which leaching fluids and sorbent particles are pumped into the underground to mobilise metal ion from the rocks, and which subsequently can be recovered, research should also target the permeability of the sorbent particles through the porous network. Therefore, some tests have been performed using a dead-end filtration set-up to assess the flow of particles through a simulated porous rock. Even though the particle size distribution is smaller than the pore size of the simulated rocks, permeability dropped drastically. Further research should focus on optimum conditions especially with regard to the size distribution and dosing of the sorbent in solution.

2 Introduction

Objectives

The objective of this task within the CHPM2030 project was the development of materials designed for target-specific mobilisation of metals in rocks.

The materials should enable a high extraction of the metals which are generated after the in situ leaching and should be able to migrate through the porous network of the rock and be recovered at the surface. The concept of the CHPM-project necessitates that these materials function under to conditions of high temperature, high pressure and in the presence of large amounts of competing and non-competing ions, which could impact their sorption behaviour.

A second important aspect of this work was the study of the behaviour of the materials during their mobilisation through a porous rock, and the impact they might have on the geological formation itself. Therefore different porous ceramics mimicking the porous architecture of real rock formation will be used in permeability experiments in order to assess the potential impact of the addition of the materials on the geological formation (and more specifically at retention and pore blockage).

The material under focus were activated carbon particles (hereafter collectively referred to as 'carbons'), with designed surface characteristics and proper size distribution. The development as such will be targeted to a combination of a porous architecture, suitable morphology and size distribution and surface characteristics.

Research strategy

The development of the carbon particles for use in mobilisation had to take several aspects into consideration.

1. Size distribution : the mean size and size distribution of the carbon particles is of importance, mainly with regard to the mobilisation of the particles through the porous network of the rock. Pore blockage by large particles or particle agglomeration will hinder flow through the pore network, will increase the injection pressures and the pressure differential between injection and production boreholes, and will inevitably mean the loss the particle(s) and the absorbed metal content
2. Porous architecture : activated carbon particles are typically characterised by their pore size, pore size distribution and high specific surface area. These characteristics are beneficial for sorption of various chemical compounds. Depending on the nature of the starting materials and the synthesis conditions (pyrolysis, activation) it is possible to design different particles having a wide range of properties.
3. Surface characteristics : although several mechanisms exist of interaction of an ion with a solid, they all are governed by the surface characteristics. Apart from the surface area available for sorption, the presence of functional groups on the surface plays a predominant role in the full sorption process. These functional groups can tune the surface to either acidic, alkaline or neutral characteristics. It is generally recognised that the sorption mechanism of activated carbons is based on the formation of a surface complex between metal ion and a surface. Metal speciation at

relevant conditions, in combination with the possibility of tuning the surface functional groups, broadens the application of activated carbons as sorbents for a wider variety of metal ions.

In order to have access to the different geological formations with different conditions and targeted metal, it is of importance to be able to tune the surface characteristics of the material.

Due to the wide variety of commercially available activated carbon particles with different specifications, no activated carbon powders were synthesized. The main focus was on the surface modification and the potential to tune the surface functional groups. Therefore, 2 strategies were selected.

1. Acid treatment, using concentrated sulphuric acid
2. Atmospheric plasma treatment, using nitrogen gas / allyl amine

These 2 approaches allowed the incorporation of either acid (carboxylic acid and sulphonic acid) or alkaline (amine, amine-like, nitrogen) functional groups. In order to assess the versatility of the methods to modify the surface of existing activated carbons, different activated carbons were selected onto which the surface modification was performed. It is important to mention that both surface modification approaches will change or transform the existing functional group into other functional groups. The newly formed functional groups on the surface were characterised with a collection of analytical tools, including titration, zeta potential measurements and elemental composition analysers.

Based on the elemental composition of the leaching solutions and in consultation with the other CHPM2030 project participants, the targeted elements were defined as the rare earth elements. The choice for targeting these elements is based on the fact that these elements are regarded as critical raw materials. In 2017, the European Commission performed a the criticality assessment to the estimates the supply risk of these elements. Rare earth elements were placed at level 5 (i.e. the highest level for all defined critical raw materials), both for heavy and light rare earth elements. Part of this high risk is due to the fact that mining rare earth elements can only be done in an economically viable way on a limited amount of minerals, due to the complex composition of the minerals (often with radioactive impurities present), the high cost for extraction and further processing and refining. As such, most of the world's supply comes from only a few sources. With more than 90 %, China has a dominant position for supplying these elements.

Also the second aspect of the criticality assessment – economic importance- the rare earth elements rank quite high. The versatility and specificity of the rare earth elements has given them a high level of technological, environmental and economic importance, also because substitutes for rare earth elements are performing inferior or are unknown. Their availability is essential for the production of high-tech and green-tech applications, which are essential for the transition towards a new and more sustainable economy. As such, any type of material or process in which rare earth elements are found, even at (very) low amounts, can be regarded as a valuable alternative source.

The chemical nature of these elements and the acidic pH range in which they occur as positively charged ions, determine the acid treated materials as the most promising. As such, these materials were the subject of further research.

Next, the developed carbon particles were assessed with regard to their sorption performance. The main sorption characteristics can be defined as

- Sorption kinetics : time required to reach equilibrium of the sorption with the solution
- Sorption capacity : maximum sorption content relative to the metal content in solution (expressed as mmol metal per weight of sorbent)
- Solid-to-liquid ratio : influence of the amount of sorbents relative to the volume of liquid (expressed as grams/millilitre)
- pH-range : influence of pH on sorption capacity

Typical for adsorption studies, these characteristics are initially investigated in idealised systems. This means that the targeted compound is present without competing ions, with well-known compositions and conditions. These experiments were meant to determine the most optimal experimental conditions (to be used within subsequent sorption experiments). Although preliminary in nature, these first experiments provided already an initial indication of the potential of the sorbent material for a specific application.

The next level within the determination of the sorption performance was the presence of competing ions. These ions can be either from the same class of elements (with similar chemical characteristics, e.g. other rare earth elements), or can be from a very different chemical nature (e.g. metal ions originating from the rock composition and liberated during leaching, e.g. iron, lead,).

In addition to the experimental conditions as expressed above, more realistic conditions for the sorption were investigated in a third set of experiments. As the CHPM concept is focussed on metal recovery under in situ conditions, sorption performance was also investigated at higher temperatures, and in presence of competing metal ions in a background of high salinity.

Apart from the development of the set of materials for metal recovery and the screening of their sorption performance, this task also comprised the mobilisation of the particles through the porous network. Therefore, permeability experiments were performed to assess the impact of the particles on the porous architecture. Due to the uncertainties about the actual porous architecture of the rock, variation of the porous network and the influence of the long term leaching on these characteristics, it was not possible to define a narrow set of parameters for the porous structure.

Therefore, porous ceramics with different pore sizes and porosities were used as simulated rocks, and were used for permeability experiments. The comparison of the permeability behaviour with water and particle loaded suspensions for different porosity and pore size levels gave indications on the impact of the particles on the flow behaviour through the porous architecture and the possible blocking of pore channels.

The following scheme represents the different stages within the development trajectory (Figure 1).

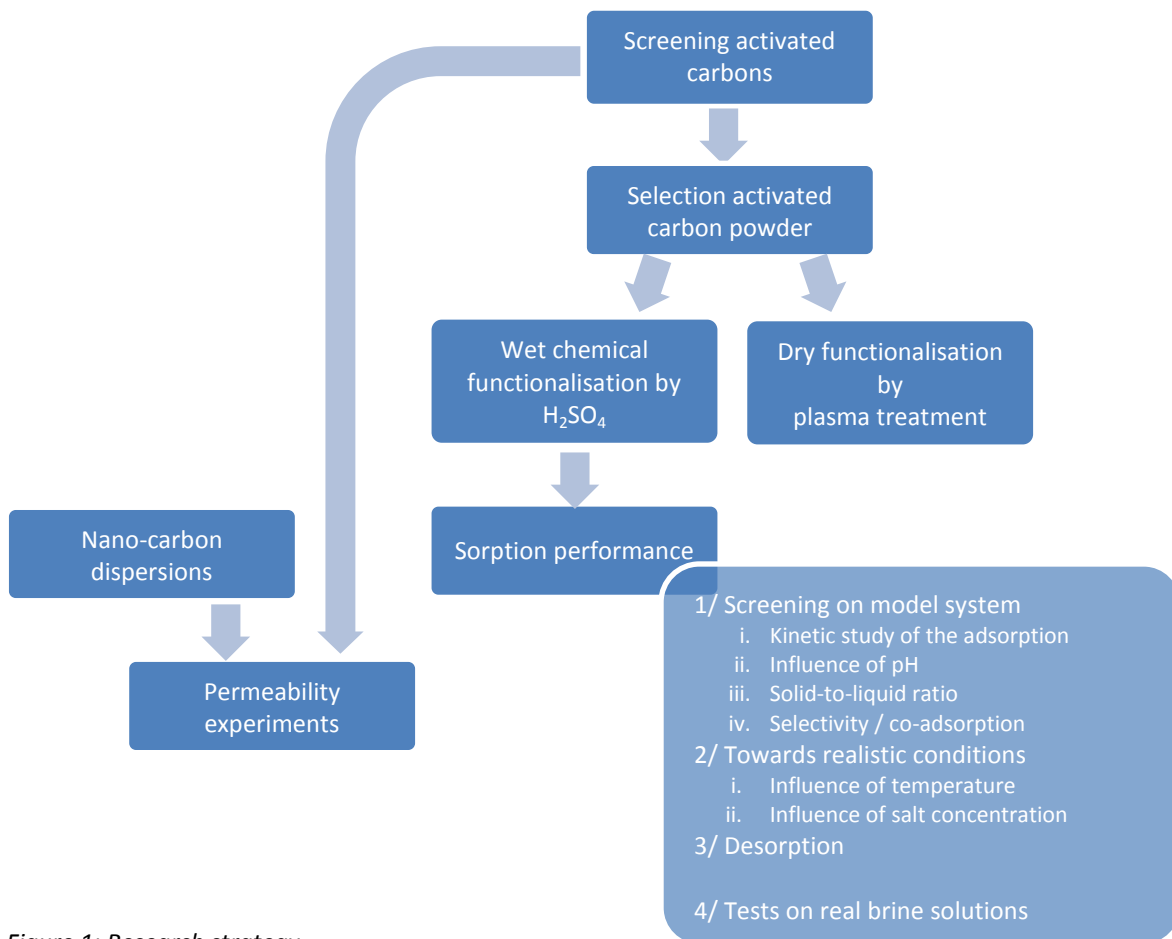


Figure 1: Research strategy

The description of the results follow the same structure as outlined in Figure 1.

- 1/ Surface modification
- 2/ Sorption performance
- 3/ Permeability experiments

3 Surface modification

Objectives

Here we describe the procedure for the selection of the activated carbon powders, and the experimental details of the functionalisation methods. The methods for the functionalisation with both acid and alkaline groups are discussed, together with a full characterisation of all samples.

The versatility of the methods will be demonstrated by the comparison of the functionalisation method on different activated carbon powders.

Screening and selection of activated carbon powders

3.1 Literature overview

1 Activated carbons

Activated carbon is widely used as solid sorbent for the removal of all kinds of contaminants from water and other process streams. In fact, it was described in the 18th century as a sorbent for the treatment of gases and the decolourisation of different aqueous solutions. Since then, the variation in activated carbon powders has increased enormously, with respect to their porous architecture and surface characteristics, leading to their use in various industrial and more advanced applications (catalysis, electrochemistry, food industry, ...).

Activated carbon is a common term used to describe a wide variety of carbon-based materials which contain a well-developed internal pore structure, combining micropores, mesopores and macropores. Chemically speaking, the structure is composed of defective hexagonal carbon layer planes (typically 5 nm wide and graphene-like sheets), in which carbon atoms are in sp^2 -hybridisation. The structure is randomly organised with pentagonal, hexagonal and heptagonal structures. Typically, the carbon content is in the range between 80 and 90 wt%. The heteroatoms are incorporated into the structure and are also bound to the periphery of the planes. The functional groups at the surface of the activated carbon, either acidic or alkaline in nature, result in a polar character of the surface.

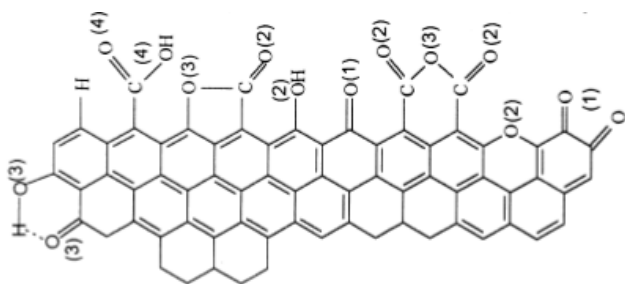


Figure 2 : Schematic representation of the structure of activated carbon, showing different oxygen surface groups.

Typically, activated carbons are produced from biomass, like wood, coal, lignite or food processing wastes such as coconut shells. The synthesis process consists of pyrolysis in inert atmosphere in the temperature

region between 600 and 900 °C, followed by an activation step to further open the porous network. Different strategies exist for the activation step, each with their own process window and properties that can be achieved. Most commonly the activation step consists in a chemical reaction (typically using metal chlorides, acids like H_3PO_4 or in alkaline conditions, e.g. the reaction with a Na or K-hydroxide), or steam/ CO_2 treatment.

The effectiveness of the materials can be attributed to a relatively unique combination of different properties like the exceptionally high specific surface areas (typically well above $1000 \text{ m}^2/\text{g}$), the high porosity, the well-developed internal pore structure and the possibility for tuning the surface chemistry with a wide range of different functional groups.

The open pore structure with pores typically ranging from micro-scale up to meso-scale, give these powders a huge surface area, which is accessible for the sorption process to occur and which can be functionalised with selective sorption sites.

From an elemental composition point of view, the activated carbons mainly consist of carbon, oxygen, hydrogen, nitrogen and sulphur. In general, the hetero-atoms are in the form of functional groups and/or atoms chemically bound to the structure. Depending on the nature of the starting material and the processing conditions (temperature and dwell time of pyrolysis, conditions for activation), a variety of chemical compositions can be obtained. Apart from the porous architecture, the nature of the chemical groups which are present on the surface will determine a predominant role in the sorption performance.

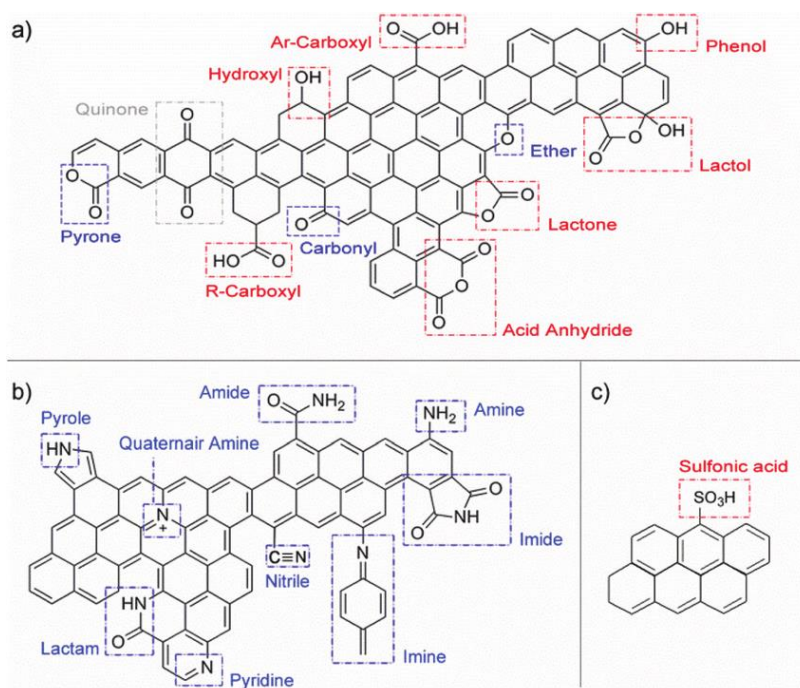


Figure 3 : Schematic view of some acidic (red) and alkaline (blue) surface groups with different heteroatoms bonded to aromatic rings on activated carbon.

As such, the surface modification strategies have been the topic of numerous scientific studies, as they are key in the development of new material concepts or in broadening the application domains for these materials.

2 Surface modification

Despite the fact that the potential of activated carbons for adsorbing a variety of compounds has been established for many years, an increasing amount of research is still being conducted into in the development of strategies for the chemical modification of its surface. The urge for new surface modification strategies originates from the need to develop activate carbons with higher affinity and/or selectivity for certain compounds, either for purification of drinking water or of a variety of industrial process streams, but also for other application (e.g. electrodes). The nature of the chemical compounds that are adsorbed onto the surface of activated carbon can be diverse, ranging from organic compounds, charged species, metal ions and gases.

Typically, the surface modification strategies can be classified according to the following scheme (Figure 4).

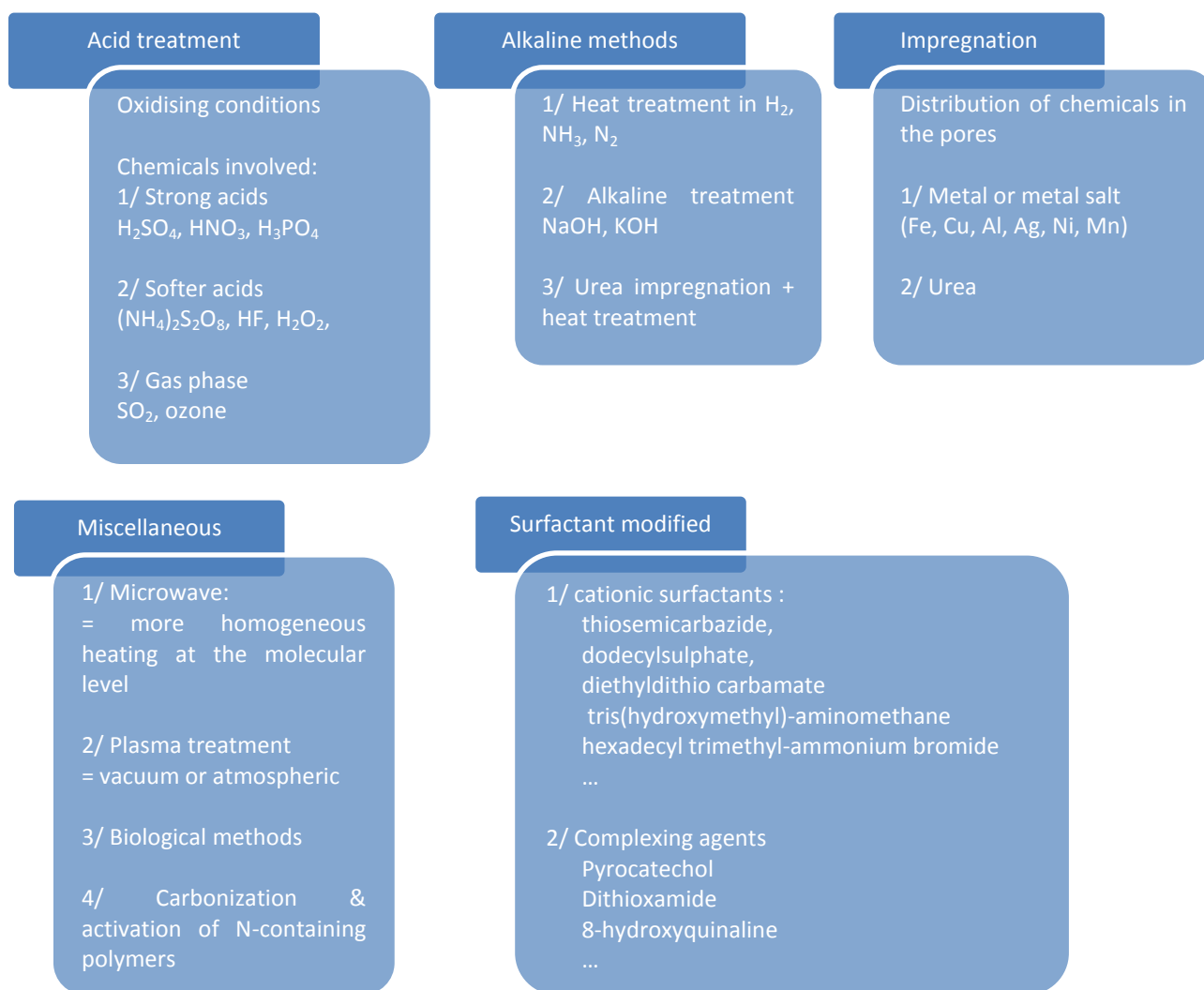


Figure 4 : Classification of the approaches for surface modification of activated carbons.

In the literature and also in this report, different term are used to express if the surface chemistry has been changed: surface modification, functionalisation and treatment.

3 Adsorption mechanism

Activated carbon and modified activated carbon are often used as sorbent materials, both for organic and inorganic compounds of diverse chemical nature. The mechanism of adsorption is determined through the chemical nature of the adsorbate and the activated carbon. Basically, one of the following mechanisms can be observed:

- 1/ π - π interactions between adsorbate and the surface of the activated carbon
- 2/ hydrogen bonding
- 3/ Van der Waals interactions
- 4/ Ion exchange

The removal from the solution and addition to the surface of the carbon particle of charged species, such as metal ions, is predominantly governed by surface complex formation between the species and the surface functional groups (Figure 5).

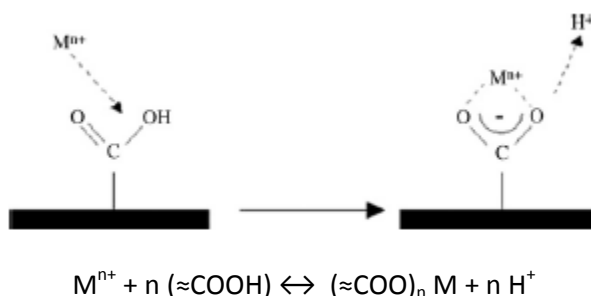


Figure 5 : Cation exchange mechanism with carbon surface carboxylic group.

The dissociation of these functional groups depends strongly on the pH of the solution and leads to a build-up of a charged interface between the activated carbon and the bulk of the solution. The formation of complexes occurs in addition to the simple ionisation of the surface functional group by the association/dissociation reaction of protons and hydroxyl ions.

As such, the adsorption of species to the activated carbon is a complex process, which is directly influenced by a number of parameters including

- pH
- ionic strength
- concentration of targeted compound
- temperature
- concentration and nature of (competing) compounds

This mechanism is the basis for the research into the surface modification of activated carbons. Tuning the nature and concentration of specific surface functional groups, tailored to a specific interaction with a compound will impact the sorption behaviour, including capacity and selectivity.

Also within this study different strategies for tuning the surface chemical composition were evaluated for the targeted metals within the brine. The specific conditions within the CHPM-context, including higher temperatures, high salinity and presence of other compounds were taken into account when designing the materials and the sorption experiments.

3.2 Screening and selection of activated carbon powders

1 Screening of activated carbons

As already stated above, the characteristics of activated carbon determine the sorption performance. In this section, the full description of the basic material characterisation is presented. The screening of the activated carbon powder was based on the combination of both structural and chemical properties of the powder. An overview of the different analytical tools used for the characterisation of the powder is presented in Table 1.

Parameter	Analytical tool	Outcome / result
Powder morphology	SEM	Image of powder particle
Pore architecture: Pore size distribution Specific surface area	N ₂ -sorption	N ₂ -sorption isotherm with calculation of specific surface area (by BET) and determination of pore size distribution
Particle size distribution	Laser diffraction (wet mode)	Particle size distribution
Point of zero charge	Zetapotential (as function of pH)	Evolution of electrical charge on particle surface as function of pH
Moisture & ash content	TGA	Weight loss as function of temperature

Table 1 : Overview of the analytical tools used for the characterisation of the activated carbon powders.

The very large variety in commercially available activated carbons necessitated narrowing down the screening process. Large scale availability, cost considerations and safety of handling were included within the selection criteria. Some experience with electrode manufacturing and surface modification on some powders limited the screening into 4 different activated carbon powders. In order to ensure comparison between the different parameters of the powders, the material characterisation was done based on a combination of analytical tools and information as supplied by the manufacturer.

The complete overview of the basic material properties is listed in Table 2.

Supplier / type	Norit - CA 1 -	Kuraray - YP-50F -	Norit - DLC Super 50 -	Norit - DLC Supra 30 -
Activation	chemical	steam	steam	steam
Powder morphology	Non-spherical	Non-spherical	Non-spherical	Non-spherical
Specific surface area [m ² /g]	1400	1500 - 1800	1660-2090	1465-2066
Total pore volume [cm ³ /g]	1.55	0.75	0.88	0.79
Micro (< 2 nm)	0.45	0.69	-	0.62-1.04
Meso (2-50 nm)	0.75	-	-	0.172-0.25
Macro (>50 nm)	0.35	-	-	-
Particle size distribution [μm]				
d ₁₀	7	2	3-5	3
d ₅₀	28	5	9-13	9
d ₉₀	75	10	50	20
Point of zero charge [PZC, pH]	2.5	-	9.9	-
Ash content [%]	2	<1	-	2
Moisture content [wt%]	11	< 3	-	3

Table 2 : Overview of material properties of the activated carbon powders.

2 Selection of activated carbons

Table 2 already demonstrates the wide variety of the properties of the activated carbon. One of the major differentiators is the strategy used for activation: either chemical or by steam. This activation step is one of the major parameters which influences the presence and nature of functional groups.

In order to prove the versatility of the surface modification strategies, the activation step of the activated carbon could be an issue. It is recognised that chemical activation is a more severe approach that will generally lead to the addition of more functional groups onto the surface, compared to the softer method of steam activation. The Norit CA-1 powder has been subjected to chemical activation. Taken into account the acidic PZC, it can be expected that the surface groups predominantly contain oxygen as hetero-element (reference is made to Figure 3).

At this stage, it is not clear whether (and to what extent) the presence and nature of pre-existing functional groups on the surface of the activated carbon plays a role in the further surface modification. Are they inhibiting the further incorporation of other functional groups ? Are they promoting the hydrophilic character of the surface and thus making the surface modification more effective ? To what extent are the surface modification approaches sensitive towards the characteristics of the substrate prior to the modification ?

As such, it is important to demonstrate the surface modification on both steam and chemically activated powders.

Also the porous architecture plays a role both in functionalisation and sorption. Micropores are defined as pores with a diameter smaller than 2 nm. These micropores create a large surface available for sorption, but might also be prone towards mass diffusion limitations, especially if a more viscous liquid is used for the surface modification. In order to include the impact of the porous architecture, activated carbons with other pore size distributions were selected.

Based on the considerations above, 2 activated carbons were selected : Norit CA-1 and Kuraray YP-50F. These activated carbons were used for testing the surface modification strategies and for further sorption studies.

3.3 Characterisation of activated carbon powders

The characteristics of the selected activated carbons were further analysed by a number of analytical tools, mainly directed towards a better understanding of the chemistry of the surface. Therefore, thermogravimetric analysis on line coupled with mass spectrometry, infrared spectroscopy, zeta potential measurements and elemental analysis were used.

1 Thermogravimetry – mass spectrometry (TGA-MS)

Thermogravimetric analysis on line coupled to mass spectrometry (TGA-MS) is a powerful analytical tool for material characterisation. The result from this analysis is the evolution of the weight (indicated as TG, %) as function of the temperature. As often the thermal reactions observed in the TGA analysis are to some extent overlapping events (kinetic effects), the interpretation is assisted by analysing the evolution of the derivative of the weight (indicated as DTG, %/min). This DTG-profile represents the rate of the material weight changes upon heating, making it easier to distinguish and deconvolute overlapping thermal events.

In this specific case, the thermal stability of the surface functional groups is lower than that of the substrate. As such, when heating a sample in inert atmosphere, the surface functional groups will decompose and the released gas from this decomposition can be identified using the MS. Comparing the TGA-MS profiles before and after modification will give information on the type and amount of created functional groups.

The temperature regions in which the specific functional groups decomposes in presented in Table 3.

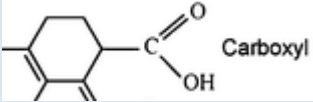
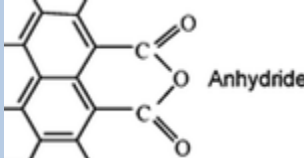
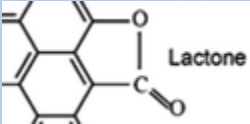
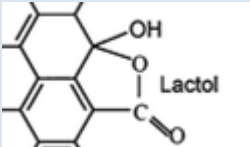
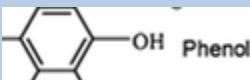
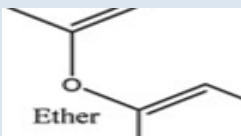
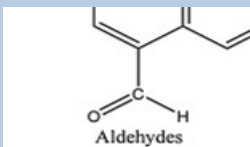
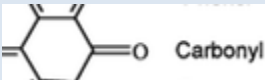
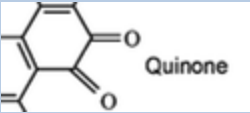
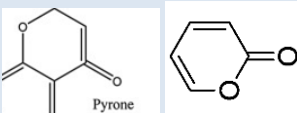
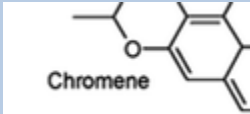
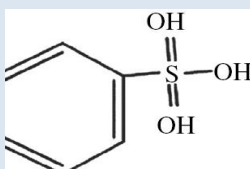
Functional group	Chemical structure	Thermal stability [°C]	Decomposition products
Carboxylic acid		250 – 400	CO ₂
Anhydride		350 - 650	CO ₂ + CO
Lactone		400 - 650	CO ₂
lactol			
Phenolic		350 – 650	CO
Ether		650 - 750	CO
Aldehyde			
Carbonyl		700 – 1000	CO
Quinone		700 – 1000	CO
Pyrone		1000 - 1200	CO
Chromene		1000 - 1200	CO
Sulphonic acid		250 - 450	SO ₂

Table 3 : Thermal stability of functional groups on activated carbon and products formed during decomposition.

The TGA-MS (Netzsch STA 449C) was performed using the following conditions: 50-150 mg of sample is heated in a flushing argon atmosphere (60 mL/min) at 10 K/min. The released gases are detected by a mass spectrometer (Omnistar, Pfeiffer vacuum, 0-200 amu), which is connected to the TGA by a heated capillary (180 °C). The mass fragments are indicated by their mass to charge ratio (m/z).



Figure 6 : TGA-MS equipment, with MS (left) and TGA coupled to a gas panel.

The results of these measurements are presented in Figure 7. For the Norit CA-1 sample, 3 distinct temperature regions were observed in which weight loss took place. Between room temperature and ~150 °C, the hydration water was released. At higher temperatures (150 – 450 °C) decarboxylation reaction occurred, releasing mainly carbon dioxide ($m/z = 44$). In the third temperature region (450 – 800 °C), surface functional groups further decomposed with the release of $m/z = 28$, attributed to the release of CO, but possibly also originating from fractions with lower molecular weight, or aliphatic compounds (C_2H_4). A very small signal attributed to the release of SO_2 ($m/z=64$, and its fragment at $m/z=48$, not shown) was observed at temperatures above 800 °C.

A different profile was noticed for the Kuraray powder. Much less weight loss over the full temperature range was observed (3 % versus 30% for the Norit), which gave a first-order indication of a lower amount of functional groups present on the surface. This feature was attributed to the steam activation. The interpretation of the MS signal is comparable to these of the Norit powder.

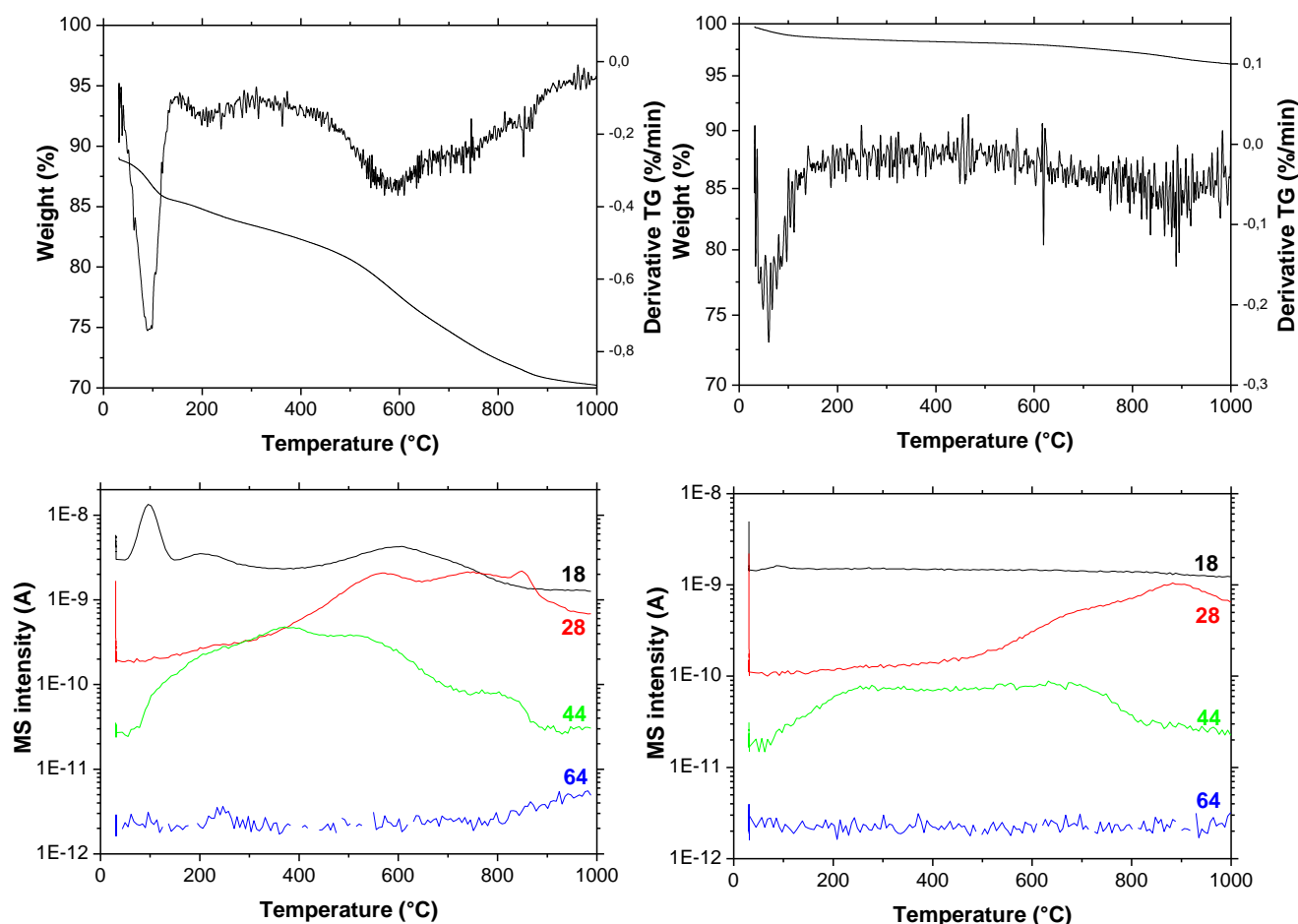


Figure 7 : TGA-MS analysis of 2 activated carbons before surface modification : Norit CA-1 (left) and Kuraray YP-50F (right).

2 Infrared spectroscopy – Attenuated total reflection (ATR)

Infrared spectroscopy is often used to characterise surface functional groups. However, an unambiguous interpretation of the spectra taken from functionalised powders is often hindered by the low amounts and/or the variety of functional groups, or the interference of bands of the substrate itself. Especially the absorbance of the carbon black itself makes the spectra not always of the best quality.

The ease of use of ATR equipment is one of the reasons for its widespread use in material science.

Figure 8 shows the ATR equipment (FTIR Nexus, Thermo Nicolet) with the diamond measuring tip onto which a small amount of powder is put.



Figure 8 : IR-ATR equipment

Figure 9 presents the ATR spectra of the activated carbons. The clear distinction between the spectra of the chemically activated carbon (in black) and the steam activated powder (in blue) was clearly noticeable within the region $2000 - 500 \text{ cm}^{-1}$. Within the spectrum of the Kuraray powder barely any peaks were noticed, indicative of the lack of surface functional groups (or at least below the detection limit of the ATR equipment).

For the Norit CA1 material, absorbance peaks are observed, at 1700 , 1580 , 1160 , 1070 and 878 - 749 cm^{-1} .

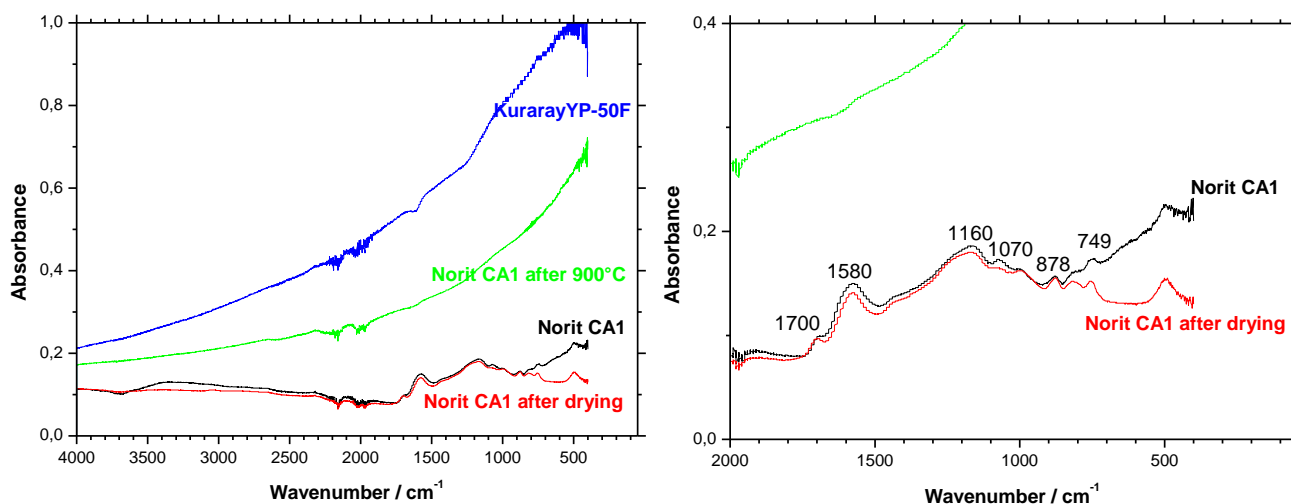


Figure 9 : IR-ATR spectra of activated carbons before surface modification.

All these absorbance bands can be attributed to different oxygen containing functional groups (Table 4).

Wavenumber [cm ⁻¹]	Identification	Functional group
1700	Stretch C=O	Lactones Carboxylic anhydrides
1580	C=O	Quinone Ceto-enol
1160 -750	C-O Stretch C=C	Ethers, lactones, phenols, carboxylin anhydrides, acids

Table 4 : Interpretation and attribution of absorbance peaks in the IR-ATR spectra of activated carbons.

3 Zeta potential measurements / Point of zero charge

The zeta potential is related to the surface charge of a given (ceramic) material, suspended in a dispersant (aqueous or non-aqueous). Its measurement gives interesting insights in the stability of a formulation and which parameters cause aggregation or flocculation of particles. Different approaches exist to measure the zeta potential. Here, the analysis is based on micro-electrophoresis (Malvern Zetasizer Nano). A voltage is applied between two electrodes, resulting in the migration of charged particles towards an oppositely charged electrode. It is the migration speed which is actually measured, using laser Doppler velocimetry and phase analysis light scattering. A laser beam is passed through the measurement cell (Figure 10) and is constantly refracted by the moving particles. The intensity of the light fluctuates with a frequency proportional to the velocity of the particles. Eventually, this velocity is calculated back to the zeta potential.

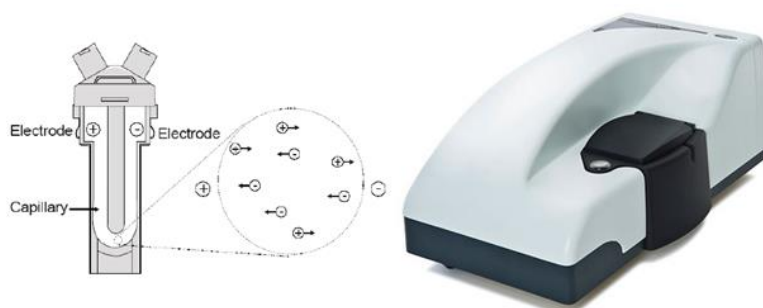


Figure 10 : Equipment used for measurement of the zeta potential.

4 Elemental analysis

Elemental analysis enables quantitative information on the elemental composition of a wide range of compounds, both organic and inorganic in nature. As the surface modification changes the elemental composition, it can be a valuable analytical tool to monitor the changes in composition with regard to carbon, hydrogen, oxygen and sulphur levels.

The principle is based on the quantitative sample digestion in high temperature (1200-1800 °C), which converts a solid or liquid sample into gaseous compounds. This gas mixture is cleaned and trapped onto a chromatographic separation column. Thermoconductivity detectors (TC) or wide-range IR detectors measure the composition the formed CO₂, SO₂, H₂ and N₂ respectively.

Figure 11 presents the equipment at VITO for elemental analysis (UniCube, Elementar).

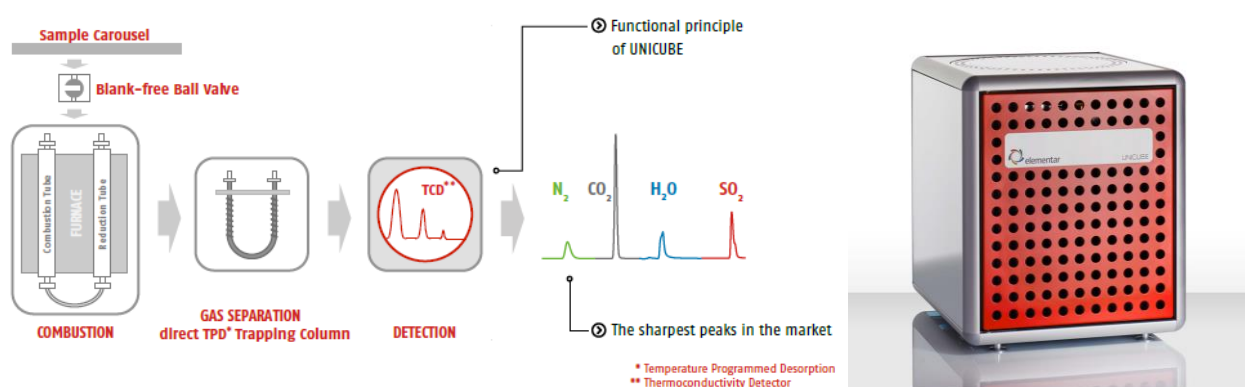


Figure 11 : Principle of the element analyser and equipment.

Table 5 presents the elemental composition of the Norit activated carbon powder, as supplied.

ID	Elemental composition [%]					TOTAL [%]
	C	S	O	H	N	
Norit_AC1	82	0.07	11	2.3	0.34	95.8

Table 5 : Elemental composition of the Norit activated carbon powder.

Surface modification of activated carbon powders

3.4 Selection of surface modification technologies

Figure 4 presented an overview of some common surface modification strategies. In order to be able to target a wide variety of metal ions, it is crucial to be able to modify the functional groups onto the activated carbons by either alkaline or acidic groups.

Therefore, 2 strategies were applied

1/ Acidic treatment :

Treating the activated carbons with concentrated sulphuric acid (H_2SO_4) has proved to be a method which can introduce sulphonic acid groups. The method is straightforward in which temperature, concentration of the sulphuric acid and the time of treatment are the main parameters in the functionalisation.

Typical sulphur content after modification is in the range between 0.5 to 1 mmol S / g sorbent. The strongly oxidising atmosphere will also lead to the co-formation of carboxylic groups. In some cases the treatment will also impact the porous nature of the activated carbon with loss of the specific surface area and a shift of the pore size distribution.

The full experimental procedure will be explained in section 3.5.

2/ Alkaline treatment

The alkaline treatment was performed by using atmospheric plasma treatment. This approach has not been fully explored yet and some literature is available. But this technology has the potential as an efficient and environmental friendly method to modify the surface characteristics of powders. The fact of being solvent-free (taking away the issues of powder recovery and drying), its compatibility with various substrates and the versatility towards different functional groups makes it a promising approach for functionalisation.

Within this study, plasma functionalisation of the 2 activated carbons is explored, aiming at the formation of amine (or other nitrogen-containing) surface groups. As such, the surface will become alkaline in nature.

The full experimental procedure will be explained in section 3.6.

An overview of the selected materials and the approaches for surface modification are presented in Figure 12.

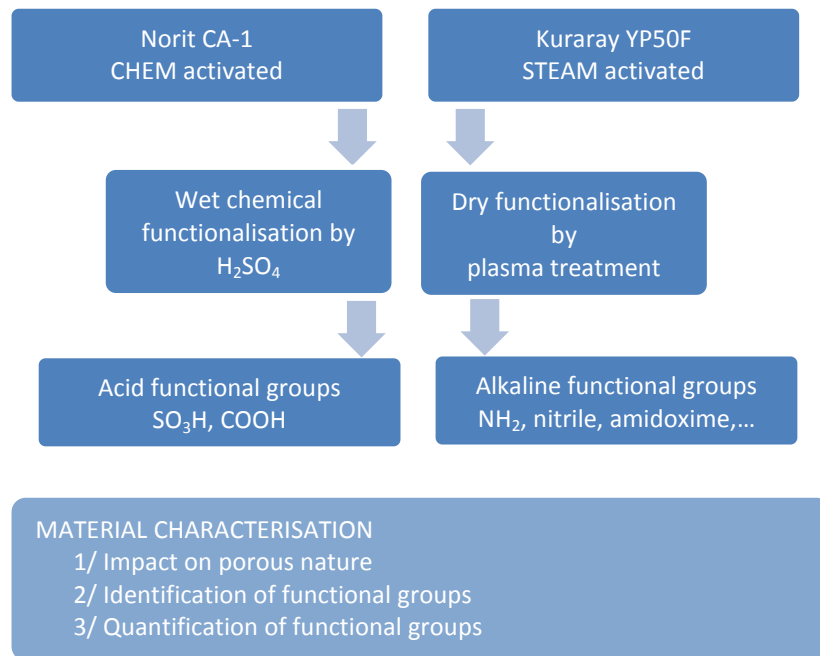


Figure 12 : Overview of materials and surface modification approaches.

3.5 Acidic treatment

1 Experimental set-up and conditions

The experimental set-up (Figure 13) for the acidic treatment consisted of a reflux set-up in concentrated sulphuric acid, at higher temperatures.

Therefore, a flask containing the activated carbon powder (15 grams) and sulphuric acid (97%, 150 mL) was connected to a water cooler [1]. This set-up was placed in an oil bath [2]. This oil bath was heated to 80 °C using a heating plate [4], controlled with a thermocouple [2]. The time of the treatment was kept constant at 3 hours.



Figure 13 : Experimental set-up for the acidic treatment of activated carbon.

2 Procedure

The following scheme presents the flow chart as used for the acidic treatment (Figure 14).

In short, 15 grams of activated carbon was put in concentrated sulphuric acid in a reflux set-up, pre-heated at 80 °C. After treatment (for 3 hours), the activated carbon was quenched in an excess ice cold water. Next, the powder was recovered by filtration and further dried (at 45 °C, overnight).

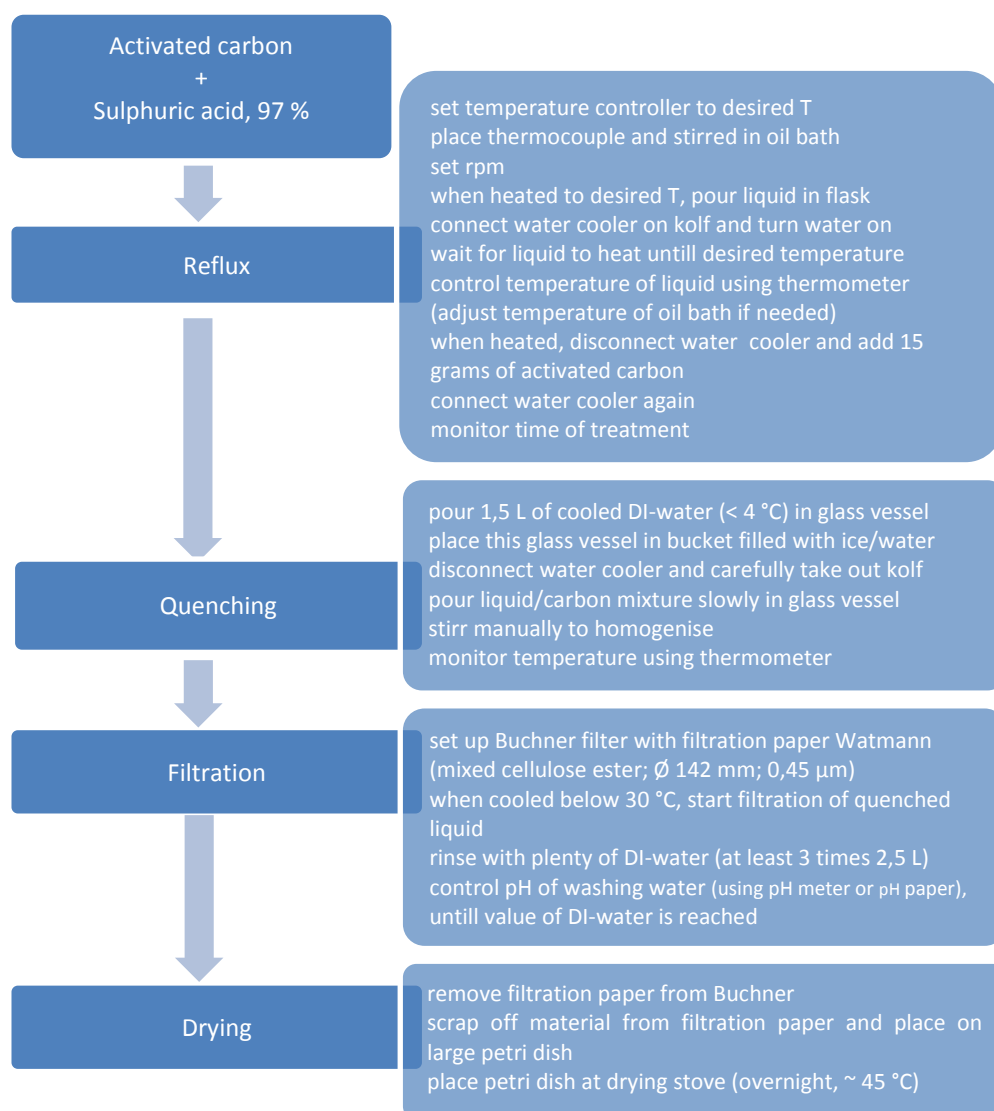


Figure 14 : Flow chart for the acidic treatment of activated carbon.

3 Materials

2 activated carbons were used for the acidic treatment. They were used without any pre-treatment prior to the surface modification treatment.

4 Materials characterisation

The analytics for the qualitative and quantitative analysis of the surface functional groups is quite challenging and interpretation might be prone to assumptions. The reason for this is the complex chemistry at the surface, the heterogeneity of the substrate and difficulties inherent to the nature of the substrate (e.g. the black colour makes it difficult for spectroscopic analysis).

In this section, results of carbon powder characterisation tests are presented, focussing on the identification and quantification of the formed surface groups. The results of both activated carbons are compared.

In the first stage, the structural characteristics before and after the treatment were measured. The data from N₂-sorption are presented in Table 6.

ID	Type Activated carbon	Surface modification	BET [m ² /g]	Micropore surface area [m ² /g]	Pore volume [cm ³ /g]	Micropore volume [cm ³ /g]
Norit_AC1	Norit_AC1	As supplied	1463	960	0,73	0,44
CHPM-17001		H ₂ SO ₄	1309	920	0,54	0,41
Kuraray_YP-50F	Kuraray_YP-50F	As supplied	1660	1595	0,11	0,67
CHPM-17002		H ₂ SO ₄	1704	1629	0,12	0,68

Table 6 : Overview of the structural parameters of the 2 activated carbons before and after acidic treatment, as measured by N₂-sorption.

As can be observed from the decrease in specific surface area (-10 %) and the pore volume (-26%), the sulphuric acid treatment impacted the structural parameters of the Norit activated carbon. Although these values seems significant, the real trend can only be judged after further research , as it must be taken into account that the N₂-sorption measurement has a typical error of about 10 %.

The steam activated carbon was more resistant towards the harsh conditions of the acidic treatment, showing no decline in pore volume or specific surface area.

TGA-MS analysis was used to give a first view on the presence of functional groups.

Figure 15 compares the TGA-MS profiles of the Norit activated carbon powder before and after functionalisation. The differences were clearly noticed in the DTG maxima : after acidic treatment, a new DTG maximum at 282 °C occurred. Also the weight loss within the temperature region between 400 – 700 had almost completely disappeared (-1.7 wt% for the sample after acidic treatment versus -10 wt% for the sample before the treatment). A small weight loss is observed between 800 and 900 °C. Also the difference in total weight loss when comparing the samples before and after treatment is quite significant: -15.2 % and -6 % respectively.

It seems the acidic treatment led to the formation of new functional groups (indicated by the presence of a new DTG-maximum), but also to the removal or transformation of the existing functional groups (as indicated by the virtual disappearance of other weight loss regions). Clearly, the mass spectrometer is a valuable tool to further interpretation of these analysis results.

The first observation is the clear release of SO₂ (as confirmed by the simultaneous evolution of m/z = 64 and 48, corresponding to SO₂ and SO respectively). This is attributed to the decomposition of sulphonic acid groups which were introduced by the acidic treatment. The maximum release of SO₂ accompanied the DTG

maximum at 282 °C. The shoulder of the $m/z = 64$ signal at higher temperatures (up to ~600 °C) could indicate the presence of another type of sulphonic acid groups (either with regard to their conformation, or location within the porous network). Apart from the indication of sulphonic acids groups, also the signal attributed to CO_2 ($m/z = 44$) clearly changed as function of the temperature compared to the untreated sample. A more distinct maximum at 282 °C was observed, possibly originating from the decomposition of carboxylic acid groups formed onto the surface. The broad band in the $m/z = 44$ signal between 350°C and 900 °C coincided partly with the evolution of with $m/z=18$ and $m/z= 28$.

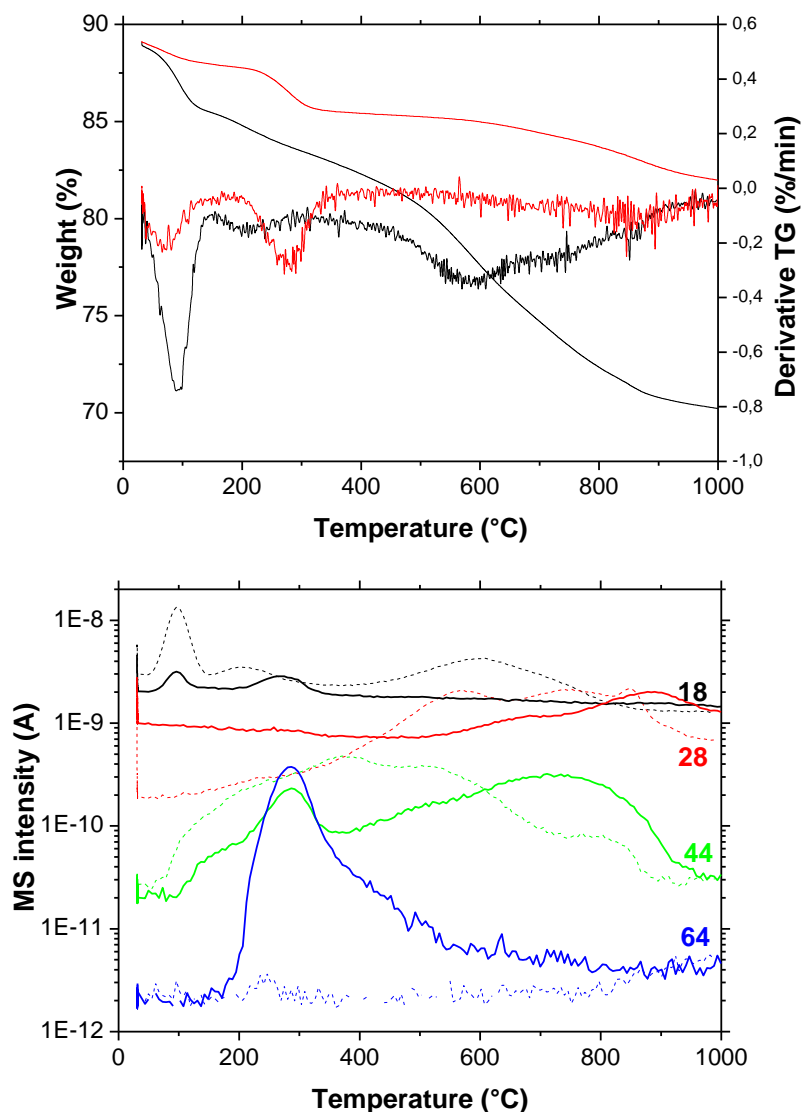


Figure 15 : TGA-MS of Norit CA1 before (black, dotted lines m/z) and after (red, full line m/z) acidic surface modification.

TGA-MS analysis was also applied on the functionalised Kuraray activated carbon (Figure 16). Again, an additional DTG maximum was observed after functionalisation. The corresponding weight loss is attributed to the decomposition of the newly formed sulphonic acid groups (as indicated by the evolution of $m/z = 64$ (SO_2)) and carboxylic acids (indicated by the evolution of $m/z = 44$ (CO_2)). A clear individual quantification of both functional groups is however not possible using the TGA-MS method. At higher temperatures (600 – 1000 °C), the weight loss increased for the Kuraray sample from 1.9 % to 3.6 % after functionalisation. The evolution of the CO_2 -signal shifted towards higher temperatures.

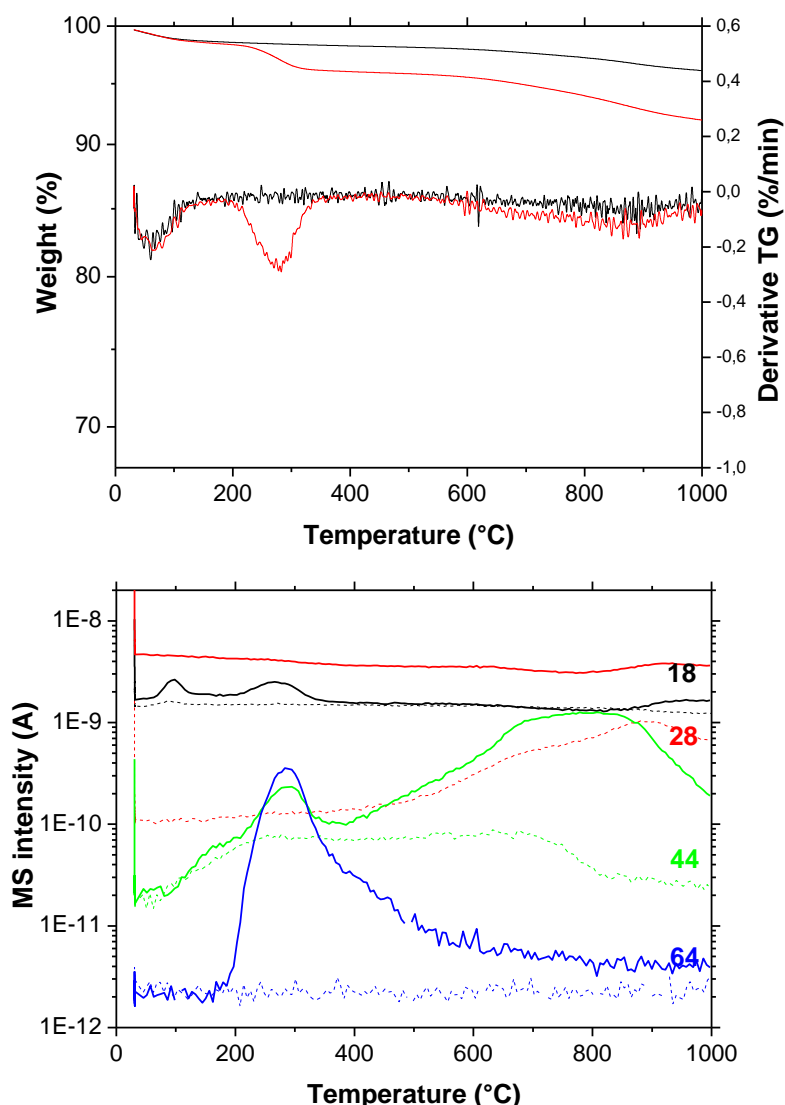


Figure 16 : TGA-MS of Kuraray YP50F before (black, dotted lines m/z) and after (red, full line m/z) acidic surface modification.

Figure 17 presents the IR-ATR spectra before and after acidic functionalisation of the Norit activated carbon powder. The broad absorbance bands in the spectrum hinder a real assessment of the changes after functionalisation : (dis)appearance of band, shift of maxima which could give unambiguous attribution of the surface chemistry. By looking at the difference spectra (Figure 17, blue) the interpretation becomes somewhat easier. The region between wavenumbers $1700 - 1500 \text{ cm}^{-1}$, only shift in position or intensity could be observed. This would indicate that the quinone and ceto-enol groups are still present after the acidic treatment. The clear increase in intensity of the absorbance ($1200 - 1100 \text{ cm}^{-1}$) points towards a higher content of carboxylic acids groups on the surface after acidic treatment. This observation is in agreement with the conclusions drawn from TGA-MS analysis (Figure 15). In the difference spectrum, a second peak is observed at $\sim 1050 \text{ cm}^{-1}$, which could originate from the vibrations of the sulphonic acid functional group. However, an unambiguous identification is difficult, since this region overlaps with vibrations from ethers, lactones, phenols and carboxylic anhydrides and acids as well.

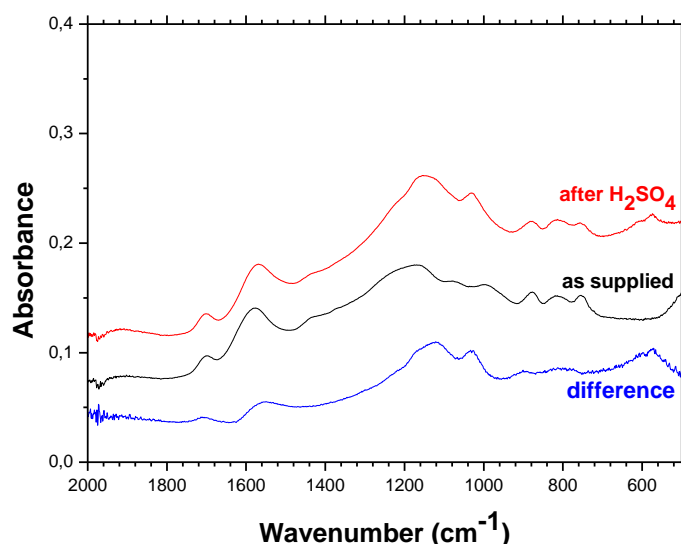


Figure 17 : IR-ATR spectra of Norit activated carbons before and after acidic surface modification.

Table 7 presents the elemental analysis of the activated carbon powder before and after acidic treatment. Before surface modification, the activated carbon had a relatively high oxygen content, originating from the oxygen containing surface groups (as also confirmed by the other analytical tools). Sulphur could not be detected in this sample (below detection limit of the equipment).

After acidic treatment, the oxygen content has increased to 14 %. The sulphur content is 2.2 %. This sulphur and part of the increased oxygen content can be attributed towards the formation of sulphonic acid groups, although an unambiguous identification towards a specific surface group is not possible based on elemental analysis.

ID	Elemental composition [%]					TOTAL [%]
	C	S	O	H	N	
Norit_AC1	82	0.07	11	2.3	0.34	95.8
Norit CA1 + H ₂ SO ₄	79	2.24	14.4	2.1	0.35	97.7

Table 7 : Elemental composition and contact pH of Norit activated carbon before and after acidic treatment.

The material characterisation clearly points to the formation of new functional groups on the surface of the both activated carbons after acidic treatment, although both materials react differently. Although the combination of analytical tools as mentioned in this section gave indications on these changes in surface characteristics, a quantitative analysis or distribution of surface groups was not possible.

3.6 Surface modification by atmospheric plasma treatment

Plasma refers to the fourth matter state, which is partially or fully ionised gas, including electrons, ions and neutral atoms and molecules. Plasma can be divided according to the temperature of the plasma (high temperature versus low temperature) or according to pressure at which the plasma is generated (vacuum plasma versus atmospheric plasma). Comparing with conventional chemical methods, plasma modification has a number of potential benefits. It is a dry method for surface functionalization, without the need for a solvent. As such, difficulties related to separation or drying of the powder which might lead to agglomeration are of no issue.

Within this study, only atmospheric plasmas (AP) are used to functionalise the activated carbon powders. The type of reactor, power of the plasma, the residence time and the type of gas (or gas mixtures) in which the plasma is generated can be the main process parameter within the process. In order to be complementary to the chemical functionalization, the study on AP-functionalisation was directed towards the creation of alkaline functional groups.

As the sorption experiments were targeted on rare earth elements which interact with acidic surface groups, no sorption tests were performed with the AP-functionalised activated carbons.

1 Experimental set-up and conditions

Within this study, the plasma treatment was done in the atmospheric plasma facilities at VITO, using a dedicated DBD (dielectric barrier discharge) system for dry functionalisation of powder materials (Figure 18). In this system, the powder is dosed in a gas flow and introduced in a plasma zone where the particles are activated. Chemical precursors can be added to modify the powder surface by applying specific functional groups. Both gaseous and liquid precursors can be used in this configuration, the latter are added as an aerosol.

For the first feasibility tests for treating the activated carbon with atmospheric plasma, a plasmazone reactor was used (Figure 18). Here, the dielectric-barrier discharge is generated between 2 electrodes which are separated by an insulating dielectric barrier (e.g. Al_2O_3 plates). By moving one of the electrodes over a powder bed, the plasma will react with the surface of the particles and functionalisation can occur.

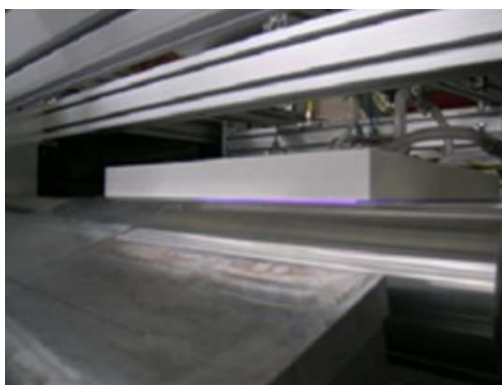


Figure 18 : Plasmazone reactor

Obviously, this type of reactor is only suited for batch-wise treatment of powder. An alternative approach for the AP-treatment is the use of a reactor, especially designed for treating powders. A schematic representation is given in Figure 19. The prototype reactor at VITO is based on a powder fall down system in which the powder is fed from the top of the cylindrical reactor. The powder is injected in a gas flow, without the use of a liquid. It is suited for the functionalization of polymer, as well as inorganic powders. A feedback loop from the reactor exit to the powder inlet system allows treating the powder in multiple passes, increasing the residence time of the powder with the plasma. For specific functionalities, the possibility to add a liquid precursor exists.

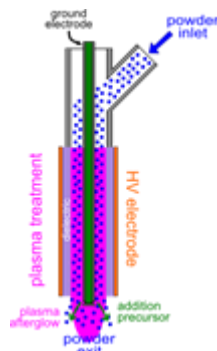


Figure 19 : Schematic representation of the AP reactor (Plazooka) used for powder functionalisation.

This option was used to introduce other types of chemistry. Aiming at the formation of amine functional groups onto the surface allyl amine is injected to the gas flow. A plasma power of 625W was used and a total N₂ flow of 130 slm. The treatment time was varied by the number of passes the powder flowed through the reactor. The exact experimental configuration for treating the activated carbon powders is described in Table 8.

ID	Activated carbon	Plasma set-up	Treatment time	Gas atmosphere
CHPM-P1	Kuraray YP50F	plasmazone	20 passes	N ₂ + allyl amine
CHPM-P2	Kuraray YP50F	plazooka	20 min	N ₂ + allyl amine
CHPM-P3	Kuraray YP50F	Plazooka	30 min	N ₂
CHPM-P4	Kuraray YP50F	plazooka	45 min	N ₂ + allyl amine
CHPM-P5	Norit CA1	plazooka	45 min	N ₂ + allyl amine

Table 8 : Experimental conditions for AP-functionalisation of activated carbon powders.

2 Materials characterisation

Similar to the chemical functionalisation, TGA-MS was used to monitor the functionalisation and to indicate which type of surface chemistry is present (Figure 20).

The AP-functionalisation of the Norit material (top left) clearly led to additional weight losses in the TGA analysis, with extra DTG maxima at 265 °C and 752 °C. Analysing the corresponding on-line mass spectrum (bottom left) identified the weight loss between 200 and 500 °C as allyl amine (with mass fragments at $m/z = 56$ and 30 (CH_2NH_2)). For reference, the mass spectrum of pure allyl amine is presented in Figure 21. Also the decomposition of carboxylic groups was identified by the evolution of CO_2 ($m/z = 44$). At higher temperatures also mass fragments of CO ($m/z=28$, possibly also C_2H_x) and CO_2 were observed, probably originating from the decomposition of the existing surface groups on the activated carbon. The additional DTG maximum at 752 °C coincided with a maximum in the release of mass fragments 44 and 30. Typically these are attributed to oxidised nitrogen compounds (NO) or amine groups (CH_2NH_2 , $\text{CH}_3\text{CH-NH}_2$). Possible mechanisms for their formation are the partly oxidation during the plasma treatment or the polymerisation of allyl amine leading to more complex nitrogen containing compounds on the surface.

Similar observations could be made for the Kuraray material after functionalisation (Figure 20, right). The additional broad DTG maximum was attributed to the release of allyl amine, with corresponding mass fragment of $m/z = 30$ and 56. The same assumptions on partly oxidation or polymerisation of the allyl amine could be drawn from these mass spectra.

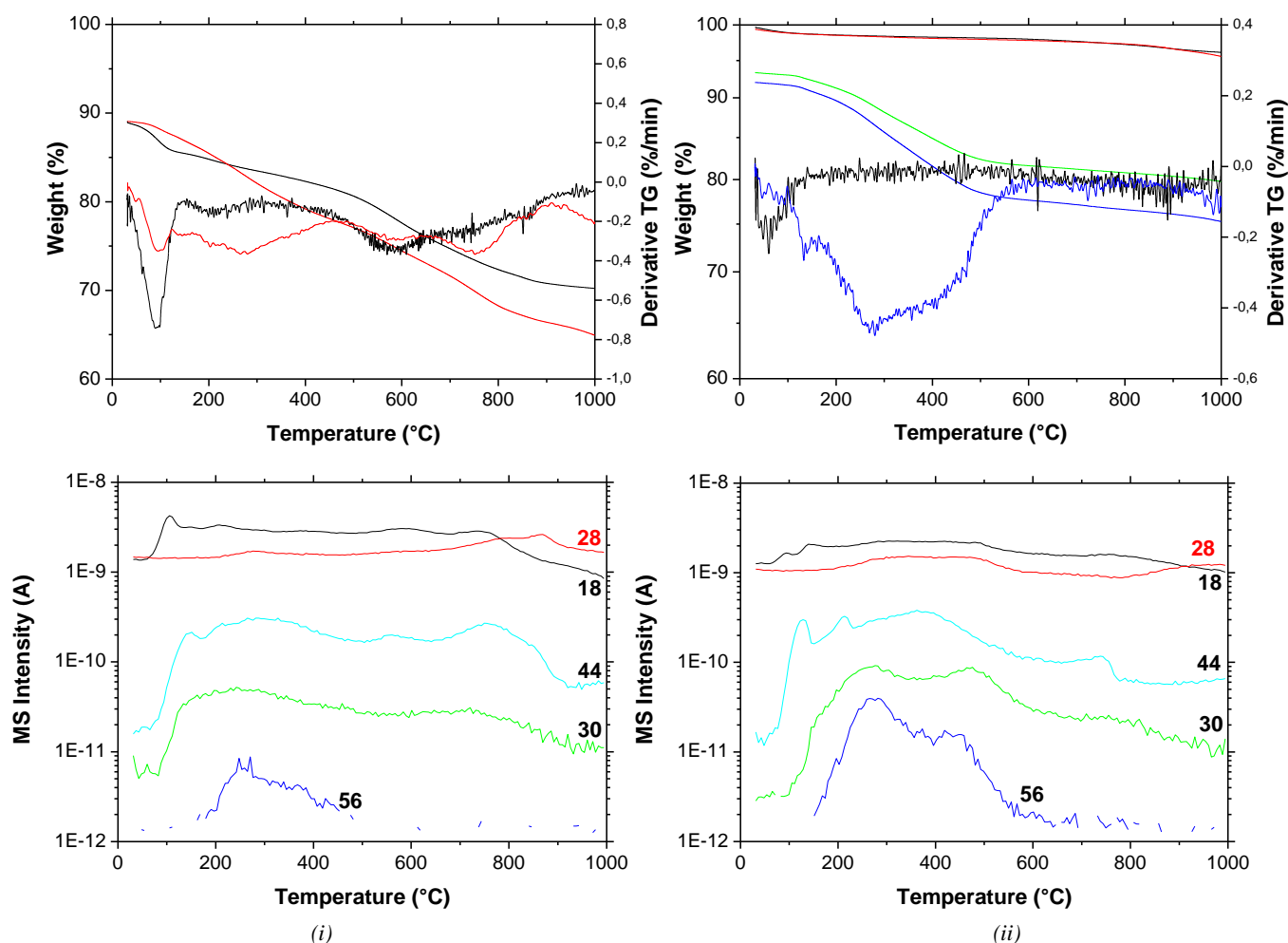


Figure 20 : TGA-MS analysis of activated carbon powders before and after AP-functionalisation (i) Norit and (ii) Kuraray.

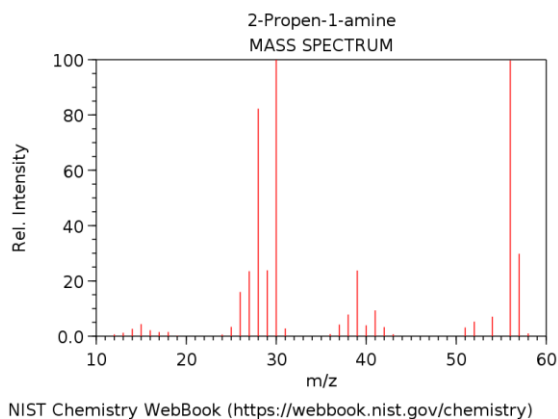


Figure 21 : Mass spectrum of allyl amine (electron ionisation, NIST webbook)

The contact pH was measured before and after the AP-functionalisation (Table 9). Both for the Kuraray and Norit powders, the contact pH shifted towards the alkaline region, due to the formation of alkaline surface groups. Especially for the Norit activated powder, the shift is remarkable.

ID	pH
Kuraray YP50F	7.9
CHPM-P1	7.5
CHPM-P3	8.8
CHPM-P4	9
Norit CA1	2.5
CHPM-P5	7.4

Table 9 : Contact pH values for activated carbons before and after AP-functionalisation.

4 Sorption performance

Objectives

This chapter describes the sorption performance for the activated carbons and their modified counterparts. The CHPM context of high pressure and temperature and the high salinity necessitates a specific approach for determining the sorption performance in more realistic conditions.

Therefore, the complexity of the sorption experiments was gradually increased from single model systems, to competitive sorption and finally using conditions at higher temperature

Research approach

The type of rock and chemical nature of the leaching fluids determine the chemical composition of the leachates, with regard to their metal content and other compounds. The presence of specific elements can influence the sorption process significantly (like e.g. salt content). The broad range of metals which are present in the leachate is exemplified in Figure 22 (input from CHPM2030 project, del. 2.2). This graph classifies the metal content in 3 major groups : common metals, “at risk metals” and the rare earth metals.

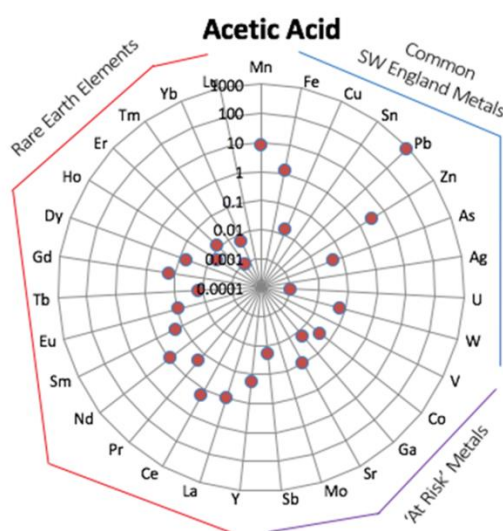


Figure 22 : Example of an elemental composition of leachate using acetic acid

As already described in section 2 (research strategy), the rare earth metals are top-ranked in the list of critical raw materials (as published by the European Commission), because of the high supply risk and their use in advanced applications. As such resources which contain this type of elements are regarded as valuable, even when the rare earths elements are present at very low concentrations.

As such, the sorption was targeted towards the removal of these elements from solution. In order to simplify the experimental conditions, neodymium was selected as a “model” rare earth element, representative for this class of elements with high chemical similarity.

In a second stage of the research, other elements were added in the solution to give a more realistic environment for the sorption. As such, competitive effect due to the presence of other rare earth elements, or due to higher concentration of more common metals was investigated.

Model sorption performance

4.1 Experimental set-up

The sorption behaviour of the activated carbons was studied by batch testing (static mode). Contrary to dynamic testing in which the liquid is flowing through a column of sorbent material, in a static test the sorbent is brought in contact with a solution for a certain time and under defined conditions. The liquid contains one or more metal ions and possibly also other compounds.

In this study the sorption was performed in glass vials, which contained a well-known amount of activated carbon and liquid of known composition (Figure 23). The liquid within the vial was stirred using a magnetic stirrer. The temperature of the lab facility was controlled to 25 ± 2 °C.



Figure 23 : Experimental set-up for measuring the sorption performance.

After the sorption experiment under a certain condition, the activated carbon was filtered from the liquid. The metal content in the liquid was measured by ICP-analysis. Depending on the concentration, the solution was diluted to fit the measuring range of the ICP-equipment. The absorbed amount of metal ions was calculated by the difference between the initial concentration in the starting solution and the concentration after filtration of the sorbent.

$$C_{\text{metal } i, \text{adsorbed}} = C_{\text{metal } i, \text{initial}} - C_{\text{metal } i, \text{after filtration}}$$

This approach and experimental set-up was used to optimise the conditions of the sorption process with regard to

- Kinetics – required time before reaching equilibrium of sorption
- Solid-to-liquid ratio – amount of sorbent per liquid ration
- pH-range
- sorption isotherm – capacity as function of concentration of targeted element

The rare earth elements present in the leachates are typified by Neodymium. $\text{Nd}(\text{NO}_3)_3 \cdot 6\text{H}_2\text{O}$ (99.9%) was selected as the starting material, due to its high solubility in water. The speciation diagram for neodymium is presented in Figure 24.

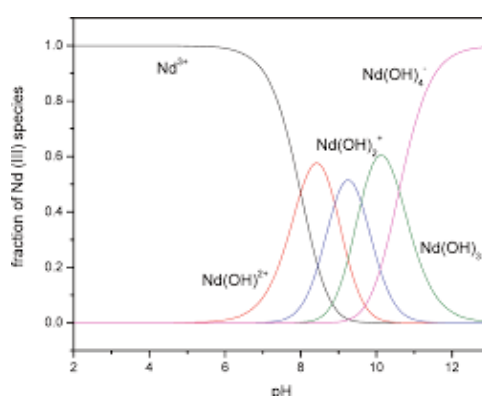


Figure 24 : Speciation diagrams for neodymium as function of the pH.

4.2 Sorption kinetics

Introduction

The sorption process is an equilibrium between the metal ion in solution and the metal ion adsorbed onto the surface (typically by complexation with the surface functional groups).



The kinetics of sorption describes the rate in which the solute is taken up by the sorbent, which in turn governs the required residence time of the sorbent with the solution. From an industrial point of view, the kinetics of the sorption are one of the most important parameters to define the efficiency of the sorption process (and the effectiveness of the sorbent material). 2 rate constants can be defined (k_1 and k_2), representing the adsorption (forward reaction) and the desorption (backward reaction). At equilibrium, the rate is the ratio of the concentration of the adsorbate in adsorbent and concentration of the adsorbate in solution.

Depending on a.o. the mechanism of sorption, the particle size and porous nature of the sorbent, the initial metal ion concentration and the solid-to-liquid ratio, the time for equilibrium can range from minutes to

several hours. Theoretical modelling of the experimental data can give insight in the underlying mechanisms. In case of strict surface adsorption, the rate should be proportional to the first power of concentration. However, when pore diffusion limits the adsorption process, the relationship between initial metal ion concentration and the rate of reaction will not be linear.

Experimental

The kinetic tests were performed in batch mode, using the Norit activated carbon before and after acidic treatment. A 20 ppm Nd^{3+} stock solution in demi-water was prepared. The exact Nd concentration of the stock solution was measured by ICP (actual value : $19350 \pm 778 \mu\text{g/L}$). The pH of the stock solution was 5.8. For the sorption tests, 50 ± 0.2 mg of sorbent was weighted and put into 20 mL solution of the Nd^{3+} stock solution. No pH adjustments were made to the solution, but the evolution of the pH was measured over time (using a SevenExcellence, Mettler Toledo equipment). The carbon suspensions were stirred at 400 rpm using a magnetic stirrer for times ranging between 10 and 360 minutes. After these time intervals, the suspensions were filtered using a polytetrafluorethene filter ($0.45 \mu\text{m}$) and the filtrate was recovered in a glass vial. The Nd content in the filtrate was analysed using ICP.

Results

Adding the activated carbon powders to the solution lowered the pH of the solution, due to the presence of acidic groups on the surface of the activated carbon.

The pH values for all samples are presented in Table 10. The pH of the suspension containing the functionalised activated carbon was ~ 2.8 , compared to 3.4 for the non-modified activated carbon. As the solid-to-liquid ratio is equal for both types of activated carbons, the lowering of the pH is indicative of the concentration of acidic groups on the activated carbon powder.

pH	10 min	20 min	30 min	60 min	120 min	240 min	360 min
Norit CA-1	3.4	3.4	3.4	3.4	3.4	3.3	3.2
H_2SO_4 functionalised	2.8	2.9	2.8	2.9	2.8	2.8	2.8

Table 10 : Evolution of pH as function of adsorption time for Norit activated carbon before and after modification.

Figure 25 presents the results of the kinetic test for the Norit activated carbon before and after acidic treatment.

On the left graph, the concentration of Nd in the filtrate is plotted for all samples. The value at time 0 min ($19350 \pm 778 \mu\text{g/L}$) represents the measured Nd concentration in the stock solution. Even at very short contact times (10 minutes), the concentration of Nd in the filtrate dropped to 350 - 650 $\mu\text{g/L}$ for the activated carbon before and after functionalisation respectively.

As the residence time of the sorbent in the solution increased (up to 6 hours), the amount of Nd in the filtrate gradually decreased further to 179 – 339 ppb. From these data, the Nd adsorption relative to the initial Nd-concentration can be calculated as

$$Nd_{\%,adsorbed} = \frac{[Nd]_{initial} - [Nd]_{residual}}{[Nd]_{initial}} \cdot 100$$

The percentage Nd adsorbed as function of the contact time of the sorbent with the solution is presented in Figure 25, right graph). Very high sorption percentages (> 96%) were obtained for both materials, even at short contact times. As the contact time increased, these levels slightly further increased to more than 98 %. The comparison of the 2 materials showed only minor differences in adsorption rate. The kinetics of the acidic functionalised material seemed somewhat slower, although more research a.o. on the reproducibility would be needed to justify this statement.

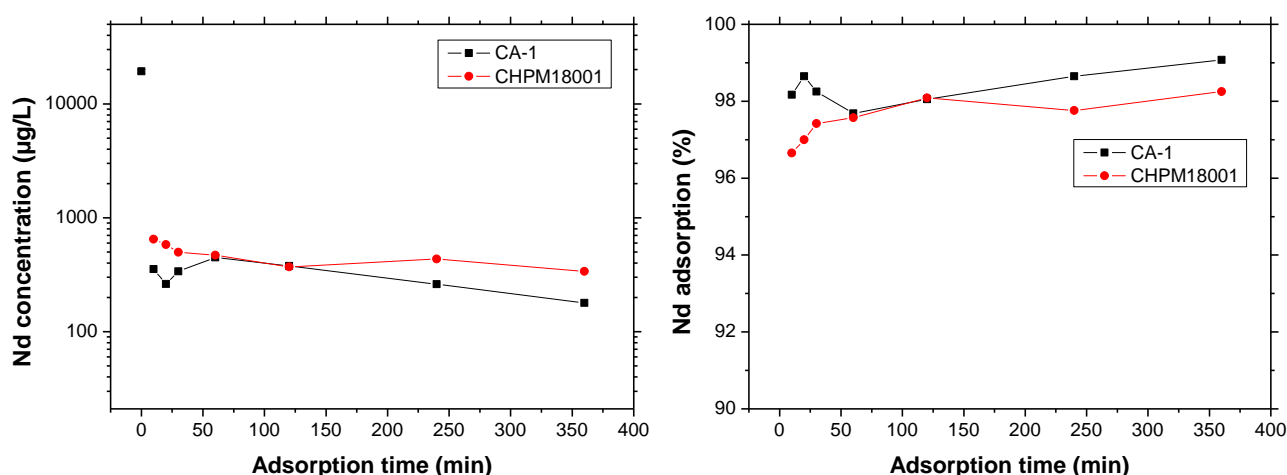


Figure 25 : Nd adsorption as function of time for activated carbon Norit before and after acidic functionalisation.

4.3 Solid-to-liquid ratio

Variations of the solid-to-liquid ratio are often used to assess the efficiency and capacity of a sorbent material. Lower amounts of sorbents within the same volume have obvious benefits for the process and costs. Also within the framework of the CHPM2030-concept, the solid-to-liquid ratio is of relevance, especially taking into account the permeability aspect of the sorbent particles through the porous network. Higher dosing of particles might lead to agglomeration and easier pore blocking.

The impact of the solid-to-liquid ratio itself on e.g. capacity is often interfered with changes in pH, as the sorbent has acidic or alkaline functional groups.

Experimental

The solid-to-liquid ratio tests were performed in batch mode, using the activated carbons before and after acidic treatment. A 20 ppm Nd^{3+} stock solution in demi-water was prepared. The exact Nd concentration of the stock solution was measured by ICP (actual value: 19650 ± 71 µg/L).

For the sorption tests, different amounts of sorbent powder was weighted and put into 20 mL solution of the Nd^{3+} stock solution. The amount of sorbent ranged from 10 ± 0.1 mg up to 500 ± 0.2 mg.

No pH adjustments were made to the solution, but the pH was measured for all samples. The carbon suspensions were stirred at 400 rpm using a magnetic stirrer for 2 hours. After this time, the suspensions were filtered using a polytetrafluorethene filter (0.45 μm) and the filtrate was recovered in a glass vial. The Nd content in the filtrate was analysed using ICP.

Results

Table 11 presents the evolution of the pH as function of the solid-to-liquid ratio for the activated carbons particles after acidic treatment. For both acidic functionalised activated carbons, the pH values decreased to the same extent ($\Delta\text{pH} \sim 1.5 - 1.8$), when dosing more sorbent material. The higher pH values for the Kuraray treated sample were indicative of a lower concentration or a different nature of acidic groups on its surface.

Sample ID	Amount sorbent [mg]	10	25	100	200	500
	S/L [g/L]	0.4	1	4	8	20
CHPM18001	Norit CA-1 + H_2SO_4	3.4	3.0	2.5	2.2	1.9
CHPM17002	Kuraray YP50F + H_2SO_4	4.4	3.8	3.2	2.9	2.6

Table 11 : Evolution of pH as function of the solid-to-liquid ratio for the activated carbons after acidic treatment.

Figure 26 (left) compares the Nd concentration as measured in the filtrate as function of the solid-to-liquid ratio for the 2 acidic functionalised activated carbon powders. The differences in sorption performance were substantial, with very low sorption capacity values the Kuraray functionalised powder (red).

The concentration of Nd in the filtrate for the Norit treated powder decreased even at low sorbent content in the suspension. Full capacity was reached from a solid-to-liquid ratio of 5. Additional dosing of the sorbent powder did not led to further reduction in the Nd concentration. Figure 26 (right) presents the percentage of Nd which was adsorbed on the activated carbon powders. Even at a solid-to-liquid ratio of 25, the Kuraray acidic functionalised powder adsorbed only 14 % of the initial Nd present. For the Norit acidic functionalised powder, the adsorption percentage reached +99 % at a solid-to-liquid ratio of 5.

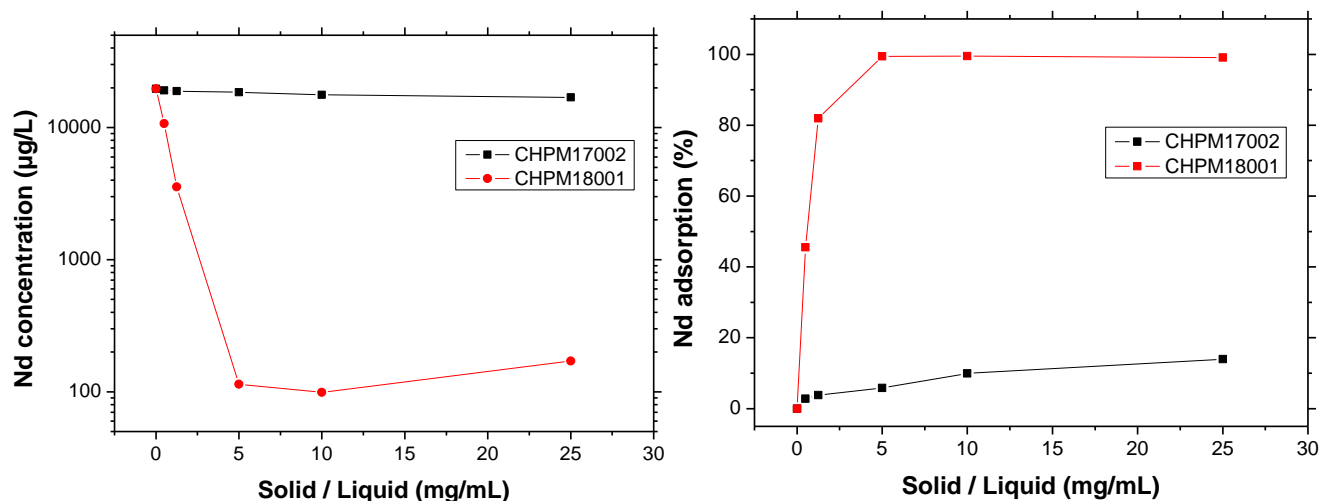


Figure 26 : Nd sorption as function of the solid-to-liquid ratio for activated carbons after acidic functionalisation.

Despite the material characterisation (section 3) gave well –grounded evidence for the formation of acidic surface groups on both functionalised activated carbons, the differences in sorption performance between the 2 powders was quite striking. Besides the surface chemistry, other characteristics of the activated carbon could be at the origin of this difference. The pore size distribution of both activated carbons is very different: the porosity of the Kuraray powder is due to only micropores (< 2 nm), while the pore size distribution of the Norit CA1 powder is much broader (from micropores, to mesopores and macropores). This porous network with smaller and larger pores could be beneficial for the functionalisation step or the sorption process, as diffusion limits will be minimized (either during the functionalisation step or in the actual sorption of the metal ion).

Another aspect to take into consideration is the hydrophilic character of the 2 activated carbon. The presence of large amount of oxygen containing surface groups renders the surface of the Norit powder very hydrophilic. The Kuraray powder is more hydrophobic (as also indicated by the low moisture content of the powder as supplied (see also Table 2).

4.4 pH range

As the sorption of metal ions on activated carbon powders is predominantly governed by their complexation with the surface groups (Figure 5), the pH plays an important role, as it regulates the dissociation of these surface groups.

Experimental

The solid-to-liquid ratio tests were performed in batch mode, using the Norit activated carbon powder before and after acidic treatment. A 20 ppm Nd^{3+} stock solution in demi-water was prepared. The pH of the stock solution was adjusted within the range pH = 2 to pH=6 (using 0.5 M NaOH or HNO_3). The exact Nd

concentrations of these solutions were measured by ICP (actual values : $19550 \pm 212 \mu\text{g/L}$ (pH=2), $19550 \pm 354 \mu\text{g/L}$ (pH=3), $19700 \pm 283 \mu\text{g/L}$ (pH=4), $19800 \pm 283 \mu\text{g/L}$ (pH=5) and $19700 \pm 283 \mu\text{g/L}$ (pH=6)).

For the sorption tests, $50 \pm 0.2 \text{ mg}$ of sorbent powder was weighted and put into 20 mL solution of the Nd^{3+} solution. The carbon suspensions were stirred at 400 rpm using a magnetic stirrer for 2 hours. After this time, the suspensions were filtered using a polytetrafluorethene filter ($0.45 \mu\text{m}$) and the filtrate was recovered in a glass vial. The Nd content in the filtrate was analysed using ICP.

Results

Figure 27 (left) shows the Nd concentration in filtrates for the Norit activated carbon before (red) and after (green) acidic functionalisation. The black line represents the Nd concentration of the stock solutions at different pH levels. The Nd concentration in the filtrates of the activated carbons decreased as pH increased, indicating that the Nd sorption process was becoming more efficient at higher pH.

The percentage Nd adsorbed as function of the pH of the solution is presented in Figure 27 (right). Very high sorption percentages ($> 90\%$) were obtained for both materials, at pH equal or higher than 3. The acidic treated sample had still a significant sorption capacity at pH 2 (almost 60 % of the initial Nd concentration is absorbed). This can be attributed to the formation of highly acidic functional groups on the surface which are still not protonated at this pH, allowing a broader pH range in which sorption could place.

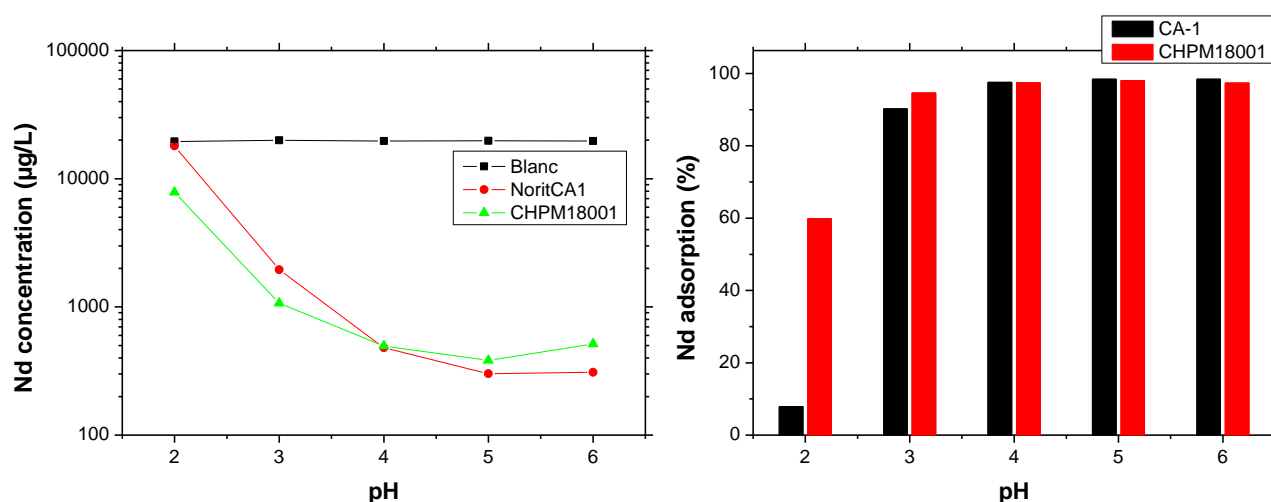


Figure 27 : Nd sorption as function of pH for activated carbon Norit before and after acidic functionalisation.

4.5 Influence of the Nd starting concentration

The capacity of the sorbent can be determined by increasing the Nd starting concentration, at equal solid-to-liquid ratio. These measurements are also the basis for the sorption isotherms and the theoretical modelling of these isotherms. They are of importance to reveal the sorption process in a more fundamental level and can give insight in the underlying mechanism of interaction of the metal ion with the surface.

Experimental

These tests were performed in batch mode, using the 2 activated carbon powders before and after acidic treatment. A 200 ppm Nd^{3+} stock solution in demi-water was prepared. From this stock solution, several dilutions were prepared, yielding Nd^{3+} solutions of 100, 50, 20, 10, 1 and 0.5 ppm. The pH of these solutions was measured (all solutions were measured to have a pH = 5.0). The exact Nd concentrations of these solutions were measured by ICP (actual values : $199500 \pm 707 \mu\text{g/L}$ (200 ppm), $101000 \pm 0 \mu\text{g/L}$ (100 ppm), $49600 \pm 0 \mu\text{g/L}$ (50 ppm), $9910 \pm 63 \mu\text{g/L}$ (10 ppm), $829 \pm 11 \mu\text{g/L}$ (1 ppm) and $285 \pm 35 \mu\text{g/L}$ (0.5 ppm).

For the sorption tests, 50 ± 0.2 mg of sorbent powder was weighted and put into 20 mL solution of the Nd^{3+} solutions. The carbon suspensions were stirred at 400 rpm using a magnetic stirrer for 2 hours. After this time, the suspensions were filtered using a polytetrafluorethene filter ($0.45 \mu\text{m}$) and the filtrate was recovered in a glass vial. The Nd content in the filtrate was analysed using ICP.

Results

Figure 28 presents the amount of Nd which was adsorbed on the activated carbon powders as function of the initial Nd concentration.

When comparing the 2 activated carbon powder before functionalisation (top left graph), a clear difference in sorption capacity was observed at higher Nd concentrations (20 - 200 ppm). At lower concentrations both activated carbon powder performed equally as good, with very high sorption percentages (+ 93 % of the initial Nd concentration is adsorbed for solutions 0.5 – 10 ppm).

As already indicated by the sorption experiments with varying solid-to-liquid ratio, the acidic treatment has an slightly negative impact on the sorption capacity. This is also observed in this experiment. For the Norit powder, the sorption capacity was lowered at higher concentrations (top right graph). For the 50 ppm initial Nd concentration, the Norit adsorbed more than 98 % of the initial Nd concentration from the solution, while for the acidic treated Norit sample this was only 65 %.

The acidic treatment on the Kuraray activated carbon (bottom left graph) had an even more pronounced effect on the sorption capacity, with sorption percentages between 5 and 25 % (0.5 – 20 ppm). A full comparison of the 2 activated carbons and the materials after acidic treatment is presented in the graph bottom right.

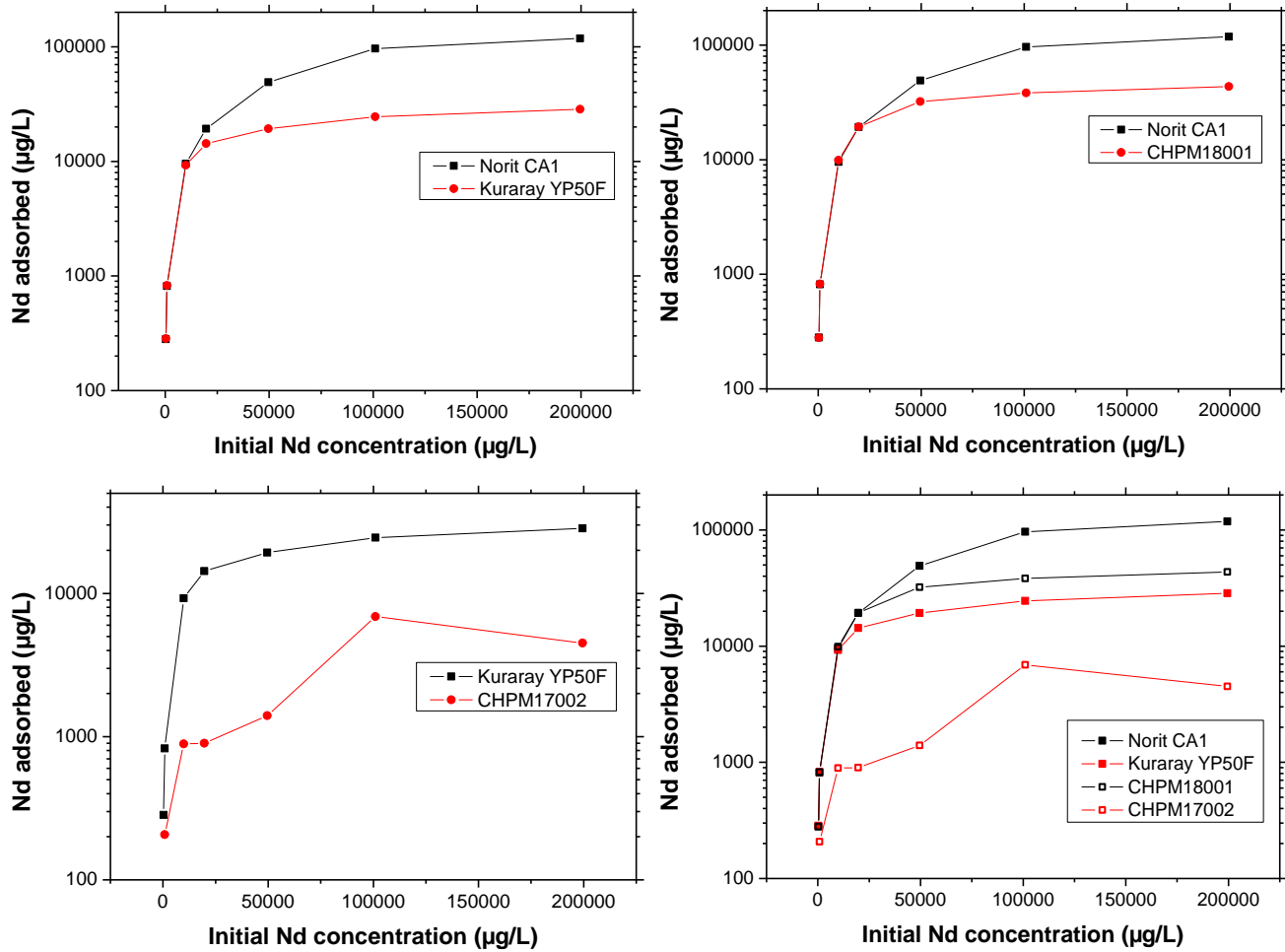


Figure 28 : Nd sorption as function of the origin Nd concentration for activated carbons after acidic functionalisation.

These graphs also form the basis for the theoretical modelling of the sorption behaviour, by fitting the data according to Langmuir, Freundlich, Tomkin or other models.

Competitive sorption performance

4.6 Competitive sorption with other rare earth elements

Experimental

These tests were performed in batch mode, using the Norit activated carbon powders before and after acidic treatment. An equimolar stock solution of Nd^{3+} , La^{3+} and Ce^{3+} was prepared starting from $\text{Nd}(\text{NO}_3)_3 \cdot 6\text{H}_2\text{O}$, $\text{La}(\text{NO}_3)_3 \cdot 6\text{H}_2\text{O}$ and $\text{CeCl}_3 \cdot 7\text{H}_2\text{O}$, corresponding to ~ 5 ppm Nd, La and Ce. The initial pH of this stock solution was 6.0. pH was adjusted in the range between 2 and 5 using 0.5 M HNO_3 . The exact Nd, Ce and La concentrations of these solutions were measured by ICP.

For the sorption tests, 100 ± 0.8 mg of sorbent powder was weighted and put into 20 mL solution of the Nd^{3+} solutions. The carbon suspensions were stirred at 400 rpm using a magnetic stirrer for 2 hours. After this time, the suspensions were filtered using a polytetrafluorethene filter ($0.45 \mu\text{m}$) and the filtrate was recovered in a glass vial. The Nd, La and Ce content in the filtrate was analysed using ICP.

Results

Figure 29 presents the metal concentration in the filtrate for the Norit activated carbon before (left) and after acidic treatment (right). The initial concentration of Nd, Ce and La of was $\sim 5000 \mu\text{g/L}$ each.

For the Norit activated carbon, the metal concentration decreased as the pH increased until a pH value of 4 was reached. At higher pH, no significant change in sorption was observed. The trend in sorption as function of pH was similar to the one observed for the single element sorption of Nd (see Figure 27, red). Notice that the absolute values of the metal concentration are different compared that of the single sorption experiment, as the experimental conditions are not identical (100 versus 50 m sorbent, ~ 5 ppm Nd, Ce, La versus 20 ppm Nd). The sorption efficiency for lanthanum was somewhat lower than these for neodymium and cerium over the full pH region: at pH 3 98 % of the neodymium present in the initial solution was adsorbed, for lanthanum the sorption percentage was almost 91 %. At higher pH, the sorption percentage increased for all metal measured to +99 % for neodymium and almost 97 % for lanthanum.

After acidic functionalisation, the sorption performance changed to some extent (Figure 29, right). At lower pH (pH 2-3), the sorption capacity was remarkably improved. At pH 2, almost 94 % of the total metal content was adsorbed, while at pH >3 , this percentage further increased to $>99\%$. No significant differences between the different rare earth elements could be noticed.

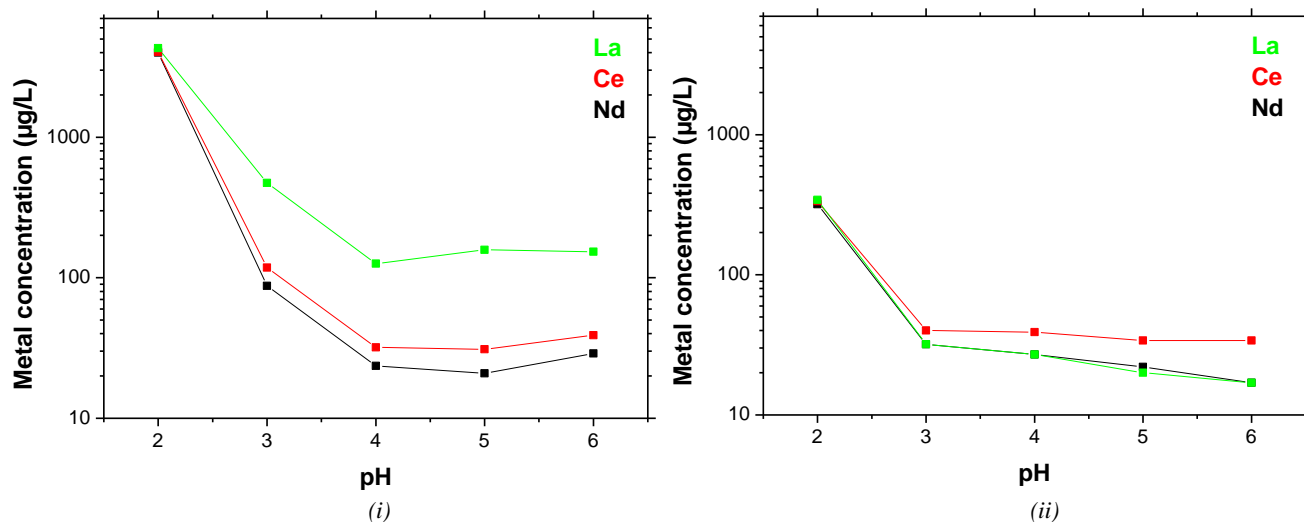


Figure 29 : Nd, Ce and La sorption as function of pH for (i) activated carbon Norit before and (ii) after acidic functionalisation.

4.7 Competitive sorption with common metal ions

The elemental composition of the leachate has shown large concentrations of more common metal ions like Pb and Zn (Figure 22). The effect of the presence of these common metal (in much higher concentrations compared to the rare earth elements) is the subject of investigation in this section.

The speciation diagram of lead is shown in Figure 30.

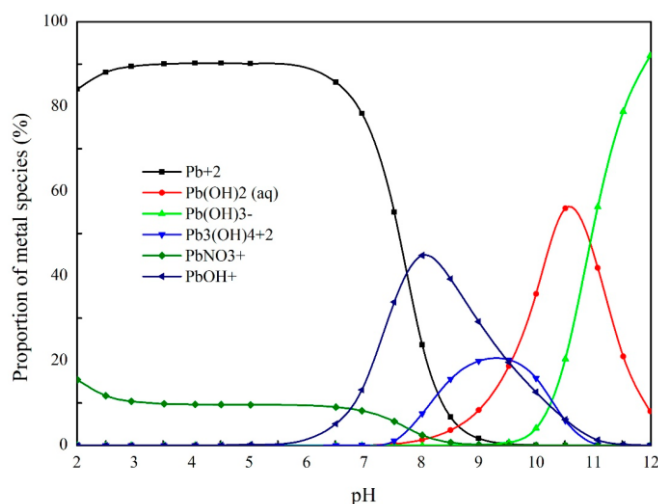


Figure 30 : Speciation diagram for Pb.

Experimental

These tests were performed in batch mode, using the Norit activated carbon powders before and after acidic treatment and the acidic treated Kuraray powder.

3 Pb^{2+} solutions were prepared by the dissolution of $\text{Pb}(\text{NO}_3)_2$. The concentration of Pb was 100, 1000 and 10000 ppm. To these solutions, Nd^{3+} , La^{3+} and Ce^{3+} were added by dissolution of $\text{Nd}(\text{NO}_3)_3 \cdot 6\text{H}_2\text{O}$, $\text{La}(\text{NO}_3)_3 \cdot 6\text{H}_2\text{O}$ and $\text{CeCl}_3 \cdot 7\text{H}_2\text{O}$ (0.0345 mM each). The exact composition of these stock solutions (Nd, Ce, La and Pb) was measured by ICP, and are reported in Table 12. The pH value for all solutions was 5.

For the sorption tests, 50 ± 0.2 mg of sorbent powder was weighted and put into 20 mL solution. The carbon suspensions were stirred at 400 rpm using a magnetic stirrer for 2 hours. After this time, the suspensions were filtered using a polytetrafluorethene filter ($0.45 \mu\text{m}$) and the filtrate was recovered in a glass vial. The metal content in the filtrate was analysed using ICP.

Result

Table 12 presents the measured metal concentrations in the filtrate for the activated carbon samples. The 3 metal containing solutions had increasing Pb content, from 100 ppm, 1000 ppm and 10 000 ppm. The measured metal concentration in the filtrate allows the calculation of the percentage adsorbed for each metal (M_i), using the following equation

$$M_{i,\% \text{ adsorbed}} = \frac{[M_i]_{\text{initial}} - [M_i]_{\text{filtrate}}}{[M_i]_{\text{initial}}} \cdot 100$$

Sample ID	Stock solution	Norit CA1		CHPM18001		CHPM17002	
	Conc. [$\mu\text{g/L}$]	Conc. [$\mu\text{g/L}$]	Adsorption [%]	Conc. [$\mu\text{g/L}$]	Adsorption [%]	Conc. [$\mu\text{g/L}$]	Adsorption [%]
Solution 1							
Pb	104500 \pm 707	44800	57	16900	84	52600	50
Ce	4895 \pm 35	1270	74	361	93	4560	7
La	4720 \pm 28	1820	61	364	92	4680	1
Nd	4945 \pm 7	1110	78	329	93	4570	8
Solution 2							
Pb	1055000 \pm 7071	783000	26	760000	28	933000	12
Ce	4980 \pm 57	4220	15	2970	40	4680	6
La	4925 \pm 21	4460	9	3090	37	4840	2
Nd	5060 \pm 28	4030	20	2830	44	4610	9
Solution 3							
Pb	10500000 \pm 0	10000000	5	10000000	5	10000000	5
Ce	5150 \pm 42	5120	1	5200	-	5230	-
La	5570 \pm 113	5600	-	5730	-	5640	-
Nd	5500 \pm 14	5330	3	5270	4	5310	3

Table 12 : Concentration of metals in filtrate and adsorption percentage of Nd, Ce, La and Pb for Norit activated carbon and the activated carbons after acidic treatment.

The impact of the presence of Pb on the sorption behaviour was quite significant. The sorption capacity for rare earth elements dropped from 96 – 99% (without lead, see Figure 29) to 61 to 74 % for the Norit activated carbon before functionalisation. The presence of sorption sites on the surface of the activated carbon powder led to quite some sorption of Pb (57 % of 100 ppm), lowering the sorption of the rare earth elements.

Further increasing the Pb concentration led to a more pronounced trend of lower capacities for the rare earth elements (9 -20 %). Co-sorption off lead was 26 % (of 1000 ppm).

The sorption behaviour for the functionalised Norit activated carbon was at lower levels of Pb different. For the solution containing 100 ppm Pb, the sorption capacity decreased only to 92 – 93 % (compared to 99% for the solutions without Pb, see Figure 29). Also the capacity for Pb is higher than that of the unfunctionalised material (84 % versus 57 %).

Also when increasing the Pb concentration to 1000 ppm, significant sorption capacity for rare earth elements is preserved for the Norit functionalised material (37 – 44%). Co-sorption of lead was in the same range as for the powder before functionalisation (28 %).

The Kuraray functionalised powder (CHPM17002) showed only affinity towards Pb (50%), with very low capacities for the rare earth elements (< 10%). The high selectivity of this powder towards Pb versus the rare earth elements could also offer benefits, by combining different sorbent materials to enhance the selectivity towards specific metal ions.

Sorption performance under more extreme conditions

4.8 Influence of temperature, salinity and competitive common metal ion

Experimental

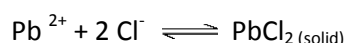
The experimental set-up for performing static sorption tests at higher temperatures is presented in Figure 31. The glass vials are placed in an aluminium heating block which ensures a homogeneous temperature distribution from the heating plate. A thermocouple is used to control the temperature within the heating block. The glass vials are closed with a Teflon stop to prevent evaporation of water.



Figure 31 : Experimental set-up for measuring the sorption performance at higher temperatures.

The sorption tests at higher temperatures were performed in batch mode, using the Norit activated carbon powder before and after acidic treatment and the Kuraray activated carbon after acidic treatment.

3 Pb^{2+} solutions were prepared by the dissolution of $\text{Pb}(\text{NO}_3)_2$. The concentration of Pb was 100, 1000 and 10000 ppm. To these solution NaCl was added, to obtain a concentration of 0.5 M. The pH of these solutions was measured : pH = 5 (100 and 1000 ppm Pb) and 3.7 (10000 ppm Pb). No pH adjustment were performed, in order to avoid the precipitation of PbCl_2 (solubility product K_s , $\text{PbCl}_2 = 1.7 \text{ E-4}$)



To these solutions, Nd^{3+} , La^{3+} and Ce^{3+} were added by dissolution of $\text{Nd}(\text{NO}_3)_3 \cdot 6\text{H}_2\text{O}$, $\text{La}(\text{NO}_3)_3 \cdot 6\text{H}_2\text{O}$ and $\text{CeCl}_3 \cdot 7\text{H}_2\text{O}$ (0.0345 mM each). The exact composition of these stock solutions (Nd, Ce, La and Pb) was measured by ICP and are reported in Table 13.

For the sorption tests, 50 ± 0.1 mg of sorbent powder was weighted and put into 20 mL of the Pb, Nd, Ce, La solution containing 0.5 M NaCl. The carbon suspensions were heated to 80°C while stirring at 400 rpm using a magnetic stirrer for 2 hours. After this time, the suspensions were filtered using a polytetrafluorethene filter (0.45 μ m) and the filtrate was recovered in a glass vial. The Nd content in the filtrate was analysed using ICP.

Results

The combined effect of temperature (80°C), salinity (0.5 M NaCl) and the presence of Pb (100 – 1000-10000 ppm) on the sorption performance is described in Table 13.

Sample ID	Stock solution	Norit CA1		CHPM18001		CHPM17002	
	Conc. [μ g/L]	Conc. [μ g/L]	Adsorption [%]	Conc. [μ g/L]	Adsorption [%]	Conc. [μ g/L]	Adsorption [%]
Solution 1							
Pb	95450 \pm 71	92000	4	91800	4	94000	2
Ce	6355 \pm 205	4860	24	4510	29	6360	0
La	6355 \pm 134	5480	14	6690	21	5040	-
Nd	5625 \pm 49	3980	29	3640	35	5340	5
Solution 2							
Pb	1002000 \pm 11314	754000	25	976000	3	960000	4
Ce	6260 \pm 57	4800	23	4890	22	6300	-
La	6490 \pm 42	5480	16	5130	21	5880	9
Nd	5615 \pm 21	3750	33	3990	29	5330	5
Solution 3							
Pb	10700000 \pm 0	10300000	4	9990000	7	10400000	3
Ce	5255 \pm 21	5310	-	5000	5	5360	-
La	4980 \pm 28	5040	-	5030	-	6630	-
Nd	5005 \pm 21	4960	1	4770	5	4970	1

Table 13 : Concentration of metals in filtrate and adsorption percentage of Nd, Ce, La and Pb for Norit activated carbon and the activated carbons after acidic treatment.(sorption conditions: 80°C, 0.5M NaCl).

The sorption percentage drastically decreased as compared to the experiment without the high salinity (Table 12), even at the lowest Pb concentration.

For Norit powders before functionalisation, the sorption percentages for the rare earth elements decreased from 60-70 % to 15 – 30 %. Also the co-sorption of Pb decreased significantly from 57 % to 4 %. At higher Pb concentrations, the sorption percentages decreased to the same extent as noticed in the sorption percentage without the presence of NaCl (16 - 33%).

For the Norit powder after functionalisation, the high sorption percentages for rare earth elements as observed in the experiment with NaCl (+92 %) dropped to 20 – 35 % in presence of NaCl (and 100 ppm Pb). At higher concentrations of Pb, the sorption performance both for rare earth elements and lead did not significantly changed, in comparison with the lower lead concentration.

The main mechanism behind the decrease in sorption capacities, as noticed for all metal ion in solution, when adding NaCl can be explain by the reduction in all electrostatic interaction due to the high ionic strength. This effect is referred to as the 'screening effect of the electrolyte'. Also, complexation of anions with the metal ion can change the speciation of the metal ions which are present in solution compared to the distribution of species present at low ionic strength.

5 Permeability

Objectives

This chapter describes the experiments performed in order to measure the permeability of different carbon particle-based suspensions through simulated porous rock samples.

Research approach

Due to the large variety in rock porosity, chemical composition, prone to fracturing etc. it is regarded as very difficult to acquire a representative view on the permeability of particle loaded suspension.

For this research, actual rocks were simulated by porous ceramics. Porous ceramic materials are available in a wide variety of chemical composition and pore architecture. Depending on the application, these materials typically can have pore size distribution from nanometers up to several millimetres in diameter. The porosity values range from 30 to more than 80 %.

Several samples were characterised with regard to their porosity, pore size distribution and interconnectivity. By selecting samples with a variety in pore size and porosity levels, the permeability of carbon particle suspensions can be assessed according to the porous architecture.

By running these tests with carbon suspensions with different particle size distribution and/or solid contents a good view could be obtained on the limits of operations and the fate of the particles within the simulated rock sample.

5.1 Experimental set-up

1 Set-up

The experimental set-up to measure the permeability is designed for measuring the permeability of thin sheet membranes. After certain adjustments, the set-up could also be equipped with 3 dimensional specimens. Basically, the set-up consists of a vessel which is capable of holding several litres of liquid (Figure 32). The vessel can be pressurized using compressed air or another gas. Typically, the pressure ranges from 1 to 3 bars. A pressure controller monitors the pressure over time. As such changes over time, due to e.g. membrane fouling or pore blocking can be recorded. The amount of liquid permeating through the membrane as function of time is recorded by computer logging of the balance which is positioned underneath the membrane sample holder.



1	Computer
2	Pressure controllers
3	Pressurized vessel
4	Outlet liquid
5	Pressure meters
6	Membrane sample holder
7	Reservoir liquid
8	Balance

Figure 32 : Experimental set-up for measuring the permeability

2 Sample holder

Typically, thin sheet, flexible membranes are measured. A specially designed sample holder prevent by passing and leakage of the liquid through the sample holder. A typical example of such a sample holder is presented in Figure 33. This sample holder is designed for measuring dead-end and in circulation filtration mode.





Figure 33 : Typical sample holder for measuring permeability of thin sheet membranes.

5.2 Screening and selection of simulated rock samples

Porous ceramics are widely available for numerous applications, ranging from biomedical to filtration media or high temperature isolation materials. Their composition and porous architecture is often designed to match specific specifications with regard to thermal conductivity, mechanical properties and machinability.

Several (commercially available) materials were screened for their use as simulated rock. As there are not any strict specifications on the porosity or pore size distribution of the material to simulate rock, it was preferred to have materials of which the pore sizes were available in a relatively broad range. The combination of SEM and Hg porosimetry was used to obtain information on the nature of the porous network.

1 List of materials to be used as simulated rock

The following materials have been used for further characterisation.

ID	Chemical composition	Available thickness [mm]	Application
1	Cordierite [SiO ₂ : Al ₂ O ₃ : MgO 5:2:2]	15	Furnace
2	Al ₂ O ₃ : SiO ₂ [70 : 30]	5	Furnace
3	Al ₂ O ₃ : SiO ₂ [xx : xx]	+ 40	High temperature isolation

Table 14 : Overview of materials used for permeability tests.

Due to the specificity of the manufacturing process of these porous ceramics, the porous parameters are often different from these of the bulk material. In order to exclude these surface effects, the porous ceramics were machined to remove the outer skin of the materials prior to use in the permeability experiments.

2 Material characterisation

This section describes the material characterisation performed to map the porous architecture of the materials which were used as simulated rock samples. The combination of Hg porosimetry and Scanning Electron Microscopy (SEM) is a powerful combination for the determination of porosity, pore size distribution and interconnectivity.

Material 1

Material 1 was a porous cordierite furnace plate. Pore size distribution was measured between 0.5 to 10 μm , with a cumulative pore volume of 150 mm^3/g (based on Hg porosimetry). SEM showed a relatively more densified structure of the top (Figure 35, top left) compared to the bulk material (Figure 35, top right same magnification). The grains within the bulk material were clearly visualised. At the outer area of the pores, sharp edges could be observed, on which particles or particle agglomerates might entangle.

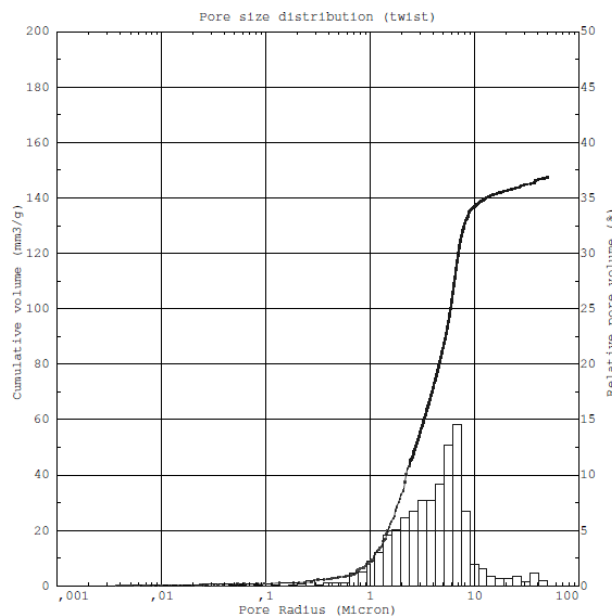


Figure 34 : Hg porosimetry analysis of sample 1.

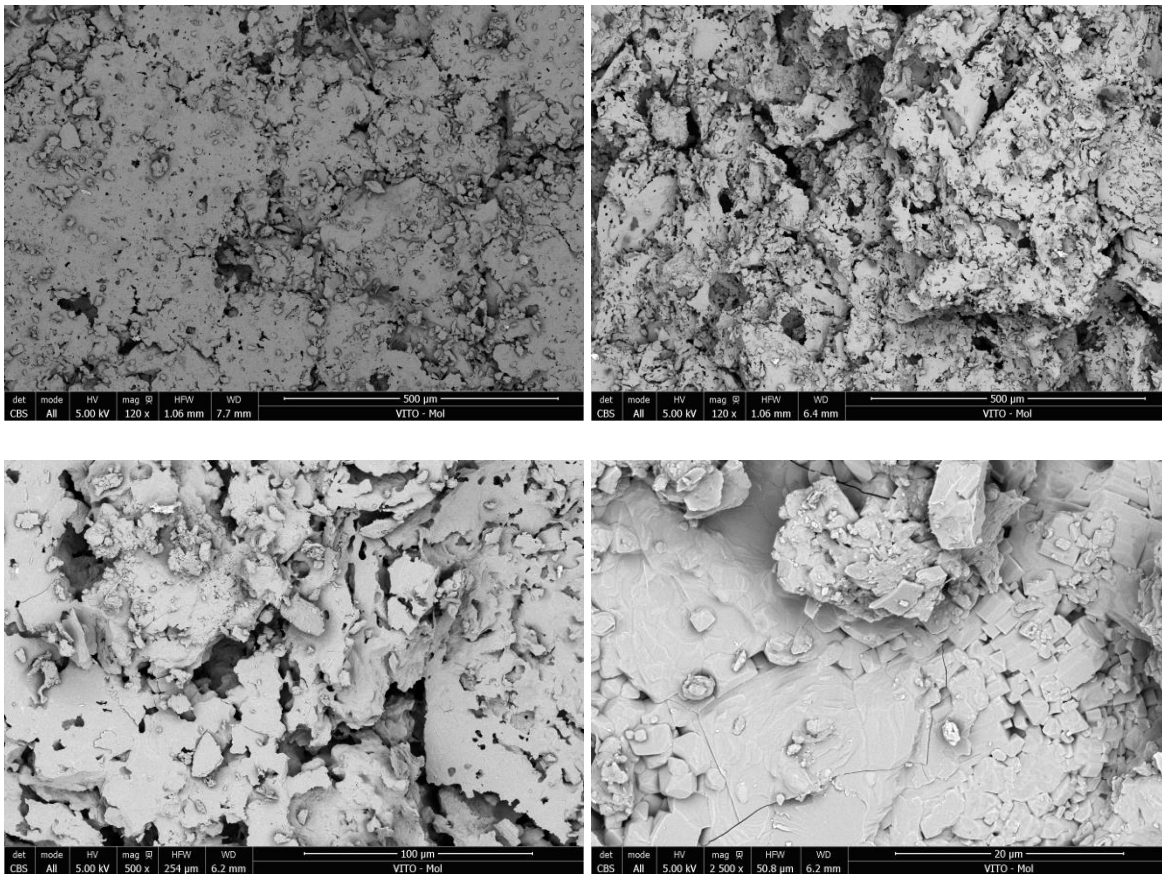


Figure 35 : SEM analysis of sample 1: surface (top left) and fracture surface (top right, bottom)

Material 2

Material 2 was a thinner glass alumina part used as a furnace shielding plate. Hg porosimetry analysis (Figure 36) showed a slightly more narrow pore size distribution (between 1 and 6 μm), and substantially lower pore volume (63 mm^3/g). The porous architecture was visualised using SEM (Figure 37).

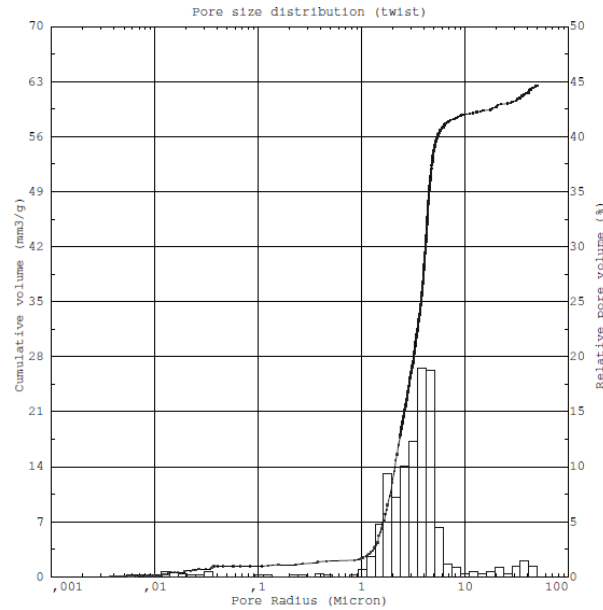


Figure 36 : Hg porosimetry analysis of sample 2.

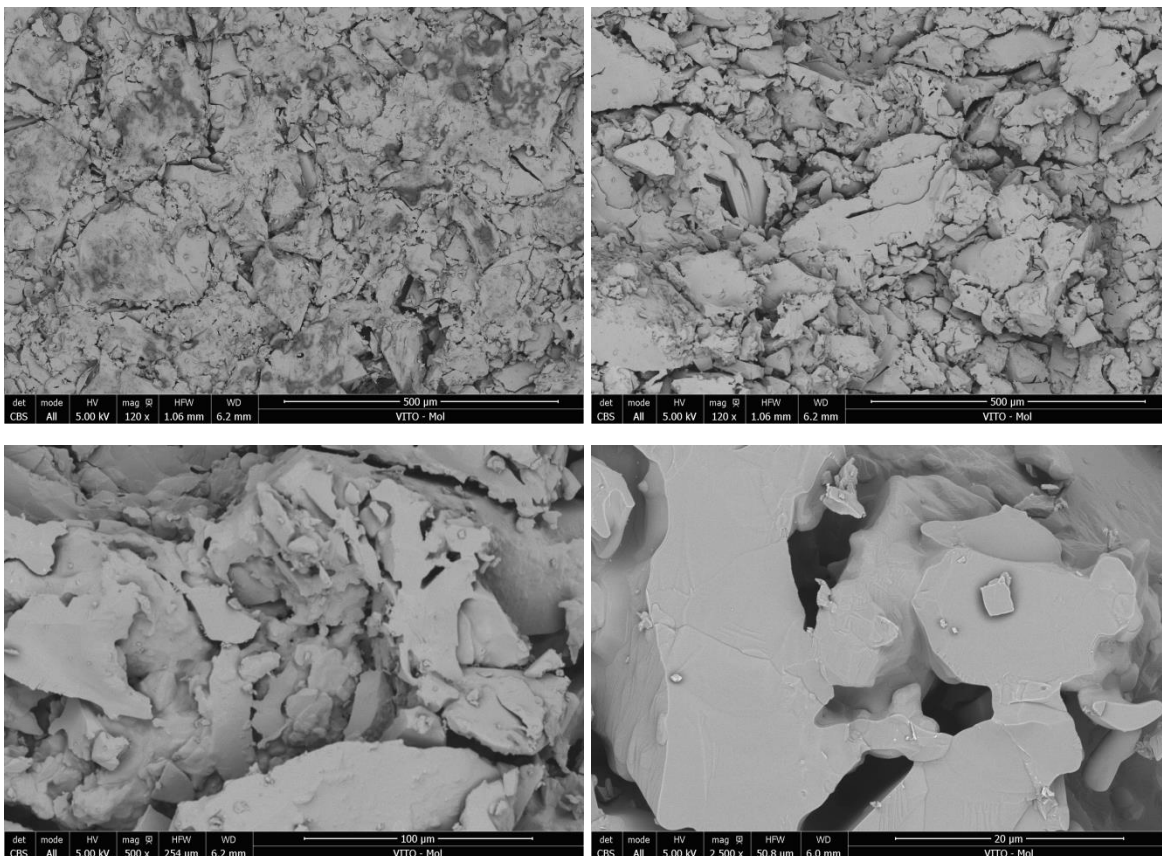


Figure 37 : SEM analysis of sample 2: surface (top left) and fracture surface (top right, bottom).

Material 3

Material 3 was a high porosity isolation material used in high temperature applications. It had by far the largest pore size distribution of the materials which were part of this screening. The largest pore sizes were outside the measuring range of the Hg porosimeter. A dual pore size distribution was observed (Figure 38), with pore size between 0.5 - 2 μm (pore volume of 110 mm^3/g) and 2 - +100 μm (exact values for pore volume are not possible, but at least higher than 270 mm^3/g).

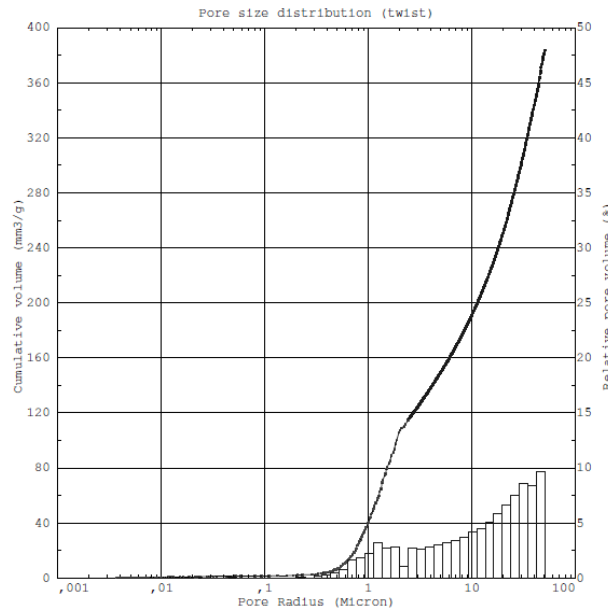
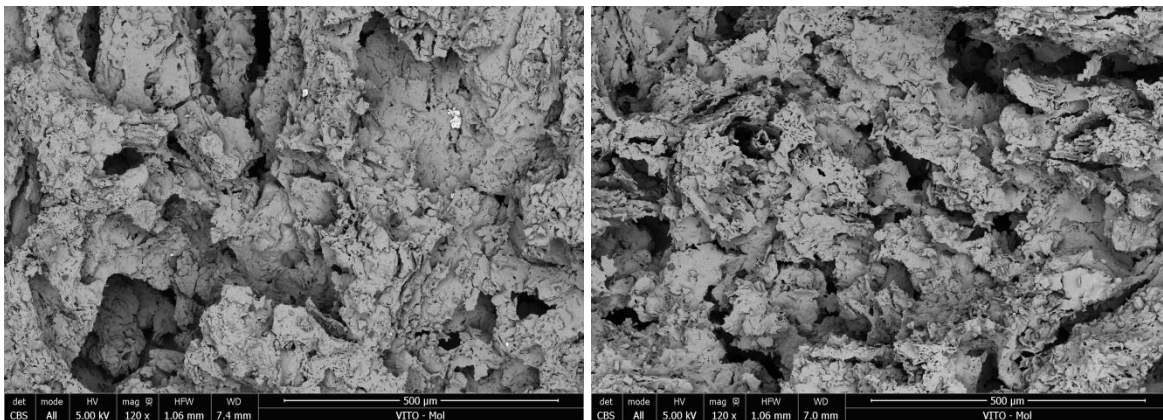


Figure 38 : Hg porosimetry analysis of sample 3.

The very open porous network is visualised by SEM (Figure 39). Common for all these materials are the sharp edges at the pore boundaries.



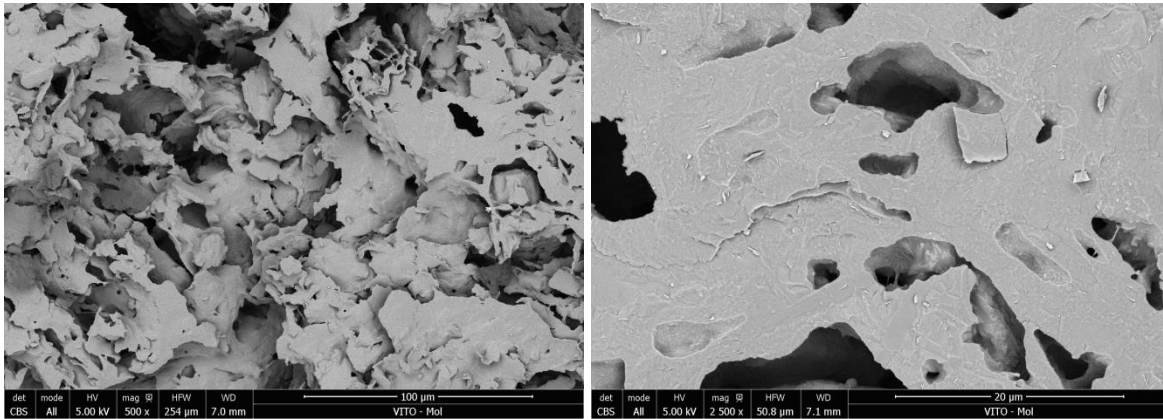


Figure 39 : SEM analysis of sample 3: surface (top left) and fracture surface (top right, bottom)

5.3 Permeability experiments

1 Procedure water permeability

The first experiments were designed to measure the water permeability using the equipment in Figure 32. The fluid reservoir was filled with 20 L of RO-water. Pressure on the reservoir was set at 1 bar.

Cylindrical shaped samples were machined with a diameter of 3 cm. A sample was placed inside the sample holder (similar to that of Figure 33) and the holder was tightened. To prevent the by-pass of the fluid along the edges of the porous ceramic, O-ring seals were placed at the top and bottom of the porous ceramic (Figure 40). The release valve was opened to allow the water to penetrate the tubing and sample holder. The permeating water was collected in a reservoir which was placed on a balance, connected to a computer for logging the data.

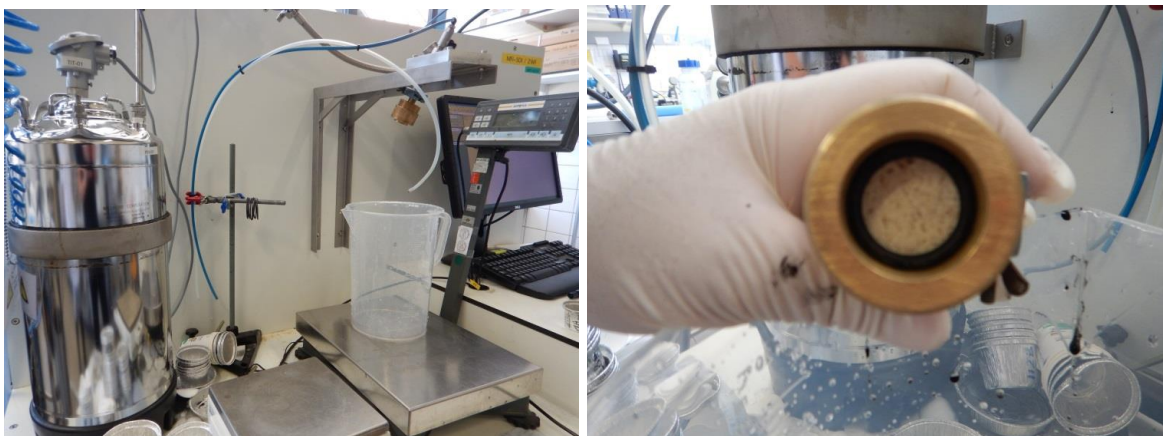


Figure 40 : Permeability set-up and mounting a porous sample in the holder

From the evolution of the weight increase as function of the time, the flux J can be calculated according to the following expression

$$J = \frac{Q}{A} = \frac{\text{permeate flow}}{\text{area of the membrane}}$$

Flux is defined as the permeate flow divided by the total membrane surface area, as shown in the formula below, and is often presented in units of liters per square meters of membrane surface area per hour. Here, the permeate flow Q is defined as the weight of water permeating the porous sample per time (in L/hr).

Figure 41 exemplifies a typical result of such a measurement, in which the weight of the permeate is measured over time. This weight increase was used to calculate the flux (red dots) over time. As can be noticed, the flux is pressure dependant : from 0 – 0.2 hours @ 1 bar and from 0.2- 2 hours @2 bars.

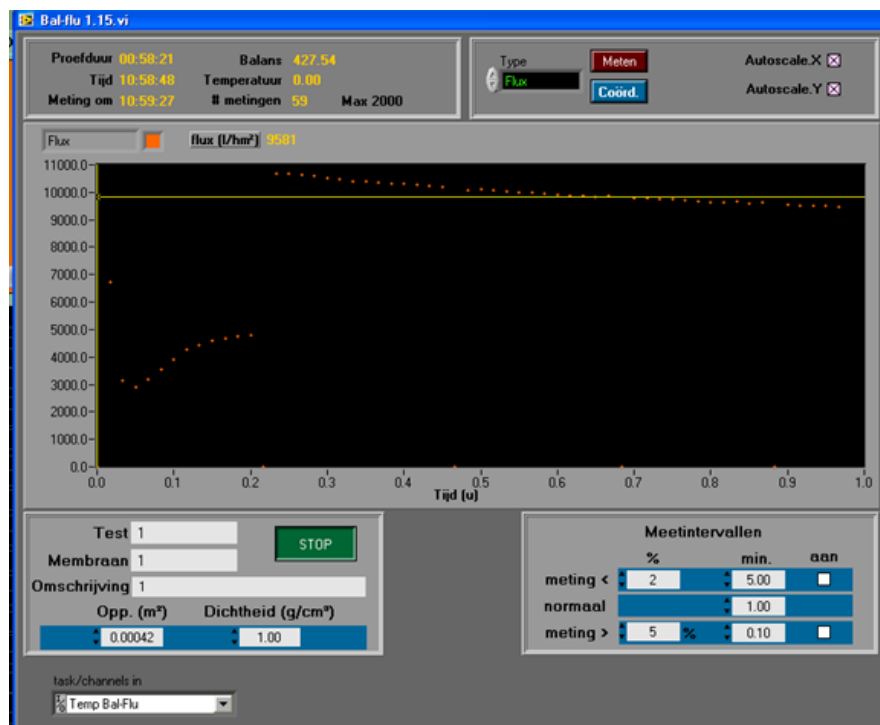


Figure 41 : Outcome of a typical permeability experiment of a porous ceramic

2 Results water permeability

The flux of the 3 samples was measured. For sample 3, a lower pressure was selected due to the very high permeability.

ID	Pressure [bar]	Flux [L/hrs, m ²]
1	2	9581
2	2	2128
3	1	317410

Table 15 : Water flux for the 3 samples

2 Results carbon suspension permeability

The very open porous network and high permeability were the reasons for selecting material 3 for the first permeability tests using a carbon suspension.

Norit activated carbon particles were dispersed in water. In total 15 L of suspension was prepared with a powder loading of 5 g/L. This value was selected based on the optimisation of the solid-to-liquid ratio for the Nd sorption experiments (Figure 26). This carbon suspension was placed inside the reservoir for the permeability test. The pressure was adjusted to 2 bars.

Figure 42 presents the evolution of the permeate flow and calculated flux for sample 3, using a carbon suspension (5 g/L Norit particles in water, at 2 bar). Over time the weight increased as water was permeating through the porous sample. However, from the trend of the flux, it could be observed that the flow of permeate is gradually decreasing (at constant pressure).

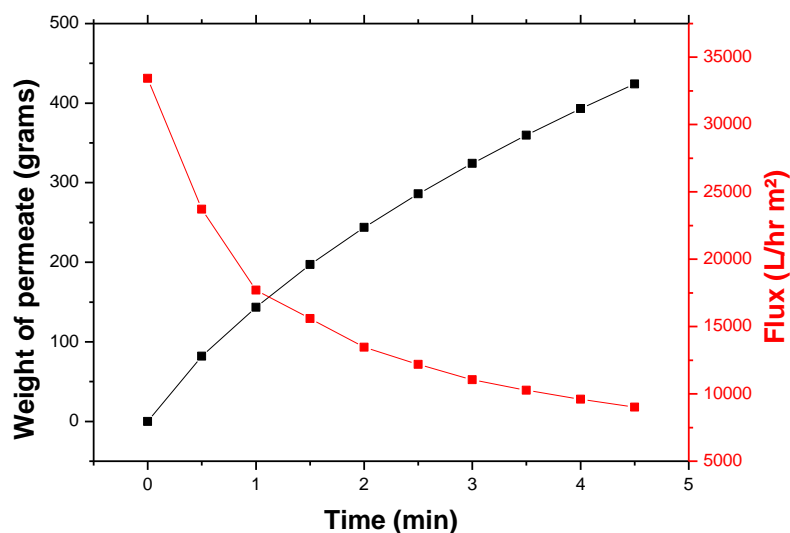


Figure 42 : Evolution of weight of the permeate and calculated flux over time for sample 3 (carbon suspension, 2 bar)

Comparing with the flux of the same sample using pure water (Table 15), a much lower value was measured for the carbon suspension. The flux decreased with almost a factor 10. Moreover, as this experiment was conducted at a higher pressure (2 bar), it must be concluded that the pores of sample 3 are being blocked from the very beginning of the experiment.

Figure 43 shows the flow of the permeate for 2 sample thickness. When the thickness of the sample was too high, the permeate flow was only drop-wise (left). Making the sample thinner increased the permeate flux (right). The permeate was in both experiments water-like, without any visual observations of particles.



Figure 43 : The flow of the permeate for sample 3 (sample thickness 2.5 cm (left) and 0.4 cm (right)).

Figure 44 shows a top view on the porous sample 3 after permeability test. Clearly carbon particles are collected at the top of the sample, without any visual indications of particle penetrating deep in the porous network

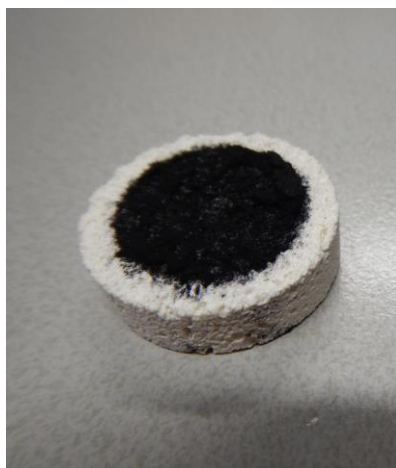


Figure 44 : Top view on sample 3 after permeability experiment.

The observation of the flux data and the composition of the permeate (with no particles present) indicated towards a filtration mechanism rather than a perfusion of particles through the porous network.

Further experiments to optimise this approach for assessing the permeability of carbon suspensions should be directed towards the dosing of the sorbent material in suspension and a reduction of the particle size distribution of the sorbent particles by milling or other de-agglomeration steps.

Also screening porous materials with larger pore sizes could be of relevance for this aspect of the study.

6 References

- AKTAS ET AL 2007: Competitive adsorption and desorption of a bi-solute mixture: effect of activated carbon type – *Adsorption* 13, 159-169
- AZIZ ET AL 2018: Effect of temperature to adsorption capacity and coefficient distribution on rare earth elements adsorptions using SIR – *Materials Science and Engineering* 349, 1-10
- ARAFAT ET AL 1999: Effect of salt on the mechanism of adsorption of aromatics on activated carbon 15, 5997-6003
- BABU ET AL 2018: EDTA-functionalized activated carbon for the adsorption of rare earths from aqueous solutions – *Industrial and Engineering Chemistry Research* 57, 1487-1497
- BHATNAGAR ET AL 2013: An overview of the modification methods of activated carbon for its water treatment applications – *Chemical Engineering Journal* 219, 499-511
- DUAN ET AL 2016: Plasma surface modification of materials and their entrapment of water contaminants: A review – *Plasma processes and polymers* 1-21
- DUSSELIET ET AL 2013 : tailoring nanohybrids and nanocomposites for catalytic applications – *Green Chemistry* 15, 1398
- ENTERRIA ET AL, Nanostructured mesoporous carbons: tuning texture and surface chemistry – *Carbon* 108, 79-102
- FARAHMAND E. 2016 : Adsorption of cerium from aqueous solutions using activated carbon developed from rice straw – *Open journal of geology* 6, 189-200
- FU ET AL 2011: removal of heavy metal ions from wastewaters: A review – *Journal of Environmental Management* 92, 407-418
- HOU ET AL 2014: Activated carbon modified with SDS as a solid phase sorbent for the separation and preconcentration of trace cadmium in water samples – *Analytical letters* 46, 1978-1990
- KANO ET AL 2017: Adsorption of rare earth elements onto activated carbon modified with potassium permanganate – *Journal of Applied Solution Chemistry and Modeling* 6, 51-61
- KOLLATH ET AL 2015: Atmospheric Pressure Plasma as an Activation Step for Improving Protein Adsorption on Hydroxyapatite Powder - *Plasma Processes and polymers* 12, 594-601
- KOMNITSAS ET AL 2017: Adsorption of scandium and neodymium on biochar derived after low-temperature pyrolysis of sawdust – *Minerals* 7, 200-217
- LOPEZ RAMON ET AL 2003: Ionic strength effects in aqueous phase adsorption of metal ions on activated carbon – *Carbon* 41, 2020-2022
- LI ET AL 2011: Maximizing the number of oxygen containing functional groups on activated carbon – *Carbon* 49, 5002-5013
- LIQIN ET AL 2014: The influence of hydroxyl-functionalised multi-walled carbon nanotubes and pH levels on the toxicity of lead – *Environmental toxicology and pharmacology*
- LIU ET AL 2010: preparation of a carbon based solid acid catalyst by sulphonating activated carbon – *Molecules* 15, 7188-7196
- MENDE ET AL 2018: The influence of salt anions on heavy metal ion adsorption on the example of nickel – *Materials* 11, 373
- MORENO-CASTILLA ET AL 2000: Changes in surface chemistry of activated carbons by wet oxidation – *Carbon* 38, 1995-2001
- PYRZYNSKA K. 2007: Application of carbon sorbents for the concentration and separation of metal ions – *Analytical Sciences* 23, 631-637

- RAJALAKSHMI ET AL 2009: Usefulness of activated carbon prepared from industrial wasate in the removal of nickel from aqueous solution – E-Journal of Chemistry 6, 361-370
- RIVERA-UTRILLA ET AL 2011: Activated carbon modifications to enhance its water treatment applications. An overview – Journal of Hazardous Materials 187, 1-23
- ROOSEN J, 2017: Recovery of critical metals from dilute aqueous waste streams by adsorption on functionalised biopolymers, PhD dissertation KULeuven
- ROOSEN ET AL 2014: Adsorption performance of functionalised chitosan-silica hybrid material towards rare earths – Journal of Material Chemistry A 2, 19415
- SAIRANEN E. 2015: Modification of carbon materials for catalyst applications, PhD dissertation Aalto University
- STEIN ET AL 2009: Functionalisation of porous carbon materials with designed pore architecture – Advanced Materials 21, 265-293
- SUDHA ET AL 2007 : Comparative study on the adsorption kinetics and thermodynamics of metal ions onto acid activated low cost pandanus carbon – E-Journal of Chemistry 4, 238-254
- TATOULIAN ET AL 2004 : plasma deposition of allyl amine on polymer powders in a fluidised bed reactor – Plasma Processes and polymers 2, 38-44
- VELISCEK-CAROLAN ET AL 2013: Selective sorption of actinides by titania nanoparticles covalently functionalised with simple organic ligands – Applied materials and Interfaces 5, 11984-11994
- XU ET AL 2008: Nanoarchitecturing of activated carbon – Advanced functional materials 18, 3613-3619
- XU ET AL 2015 : Adsorption of rare earths using an efficient sodium alginate hydrogel crosslinked with polyglutamate – PLoS One 10(6)
- YIN ET AL 2007: Review of modifications of activated carbon for enhancing contaminant uptake from aqueous solutions – Separation and purification technology 52, 403-415
- YANTASEE ET AL 2004: Electrophilic aromatic substitutions of amine and sulphonate onto fine-grained activated carbon for aqueous –phase metal ion removal – Separation Science and Technology 39, 3263-3279

7 Conclusions

The CHPM technology relies on the release and recovery of metals within the subsurface. Here we report the results of the development of carbon particles with designed surface chemistry to enhance the sorption of the metal ions which are released.

This research is part of work package 2 within the CHPM2030 project.

The research focussed on the development of strategies to tune the surface chemistry of carbon particles with different surface groups, enabling the specific sorption of valuable metals. As targeted metals and conditions within the subsurface might vary, both strategies were selected to be complementary with regard to the acidity /alkalinity of the surface groups.

The developed materials have been fully characterised with regard to their materials properties as well as their sorption behaviour.

The major conclusions from this can be formulated as follows

- The variety in activated carbon characteristics with regard to their porous nature and surface chemistry result in diverse sorption behaviour of these materials for metal ions. The most optimum material showed very fast sorption kinetics (< 10 min) with high adsorption percentage (+90 %) over a relatively broad pH range (pH 3 - 6).
- Sulphuric acid treatment of the activated carbon particles leads to changes in surface chemistry, with the formation of acidic oxygen-containing surface groups as well as sulphonic acid groups. The combination of analytical tools was indispensable to get a better view on the distribution of functional groups, although a quantitative distribution of all functional groups was not possible.
- The characteristics of the activated carbon particles are a major factor in the functionalisation mechanism, impacting a.o. the preservation of the porous nature, the type and concentration of functional groups
- As such, also the impact of the functionalisation on the sorption performance is evident. In general, the sorption capacity decreased slightly, but it was compensated by a broader pH range in which the sorption takes place with high adsorption percentage (+90% at pH 2).
- Also when considering competition with other rare earth elements or more common metal ion present at much larger concentration the surface functionalisation could be beneficial. Sorption percentages for rare earth elements were significantly higher for the functionalised powder in presence of lead (+90 % versus 60-80 %, for 100 ppm Pb).
- At higher concentrations of Pb, the sorption percentage of rare earth elements further decreased, but remained significantly for the functionalised powders (~40 % versus 15 %).
- As the experimental conditions for selective sorption became much harsher (i.e. high concentrations of competing ions and high salinity), the sorption capacity further reduced to 15 – 35 %.
- The first experiments on the permeability revealed that at the current conditions clogging of the surface pores occurred almost instantly. The permeability testing needs further optimisation with regard to the experimental conditions, including an optimisation of the dosing of the sorbent, a further screening of materials with larger pores and the influence of the particle size of the sorbent by milling or deagglomeration.